Organ doses for reference pediatric and adolescent patients undergoing computed tomography estimated by Monte Carlo simulation

Choonsik Lee[a)]
Division of Cancer Epidemiology and Genetics, National Cancer Institute, National Institute of Health, Bethesda, Maryland 20852

Kwang Pyo Kim
Department of Nuclear Engineering, Kyung Hee University, Gyeonggi-do, Korea 446906

Daniel J. Long and Wesley E. Bolch
J. Crayton Pruitt Family Department of Biomedical Engineering, University of Florida, Gainesville, Florida 32611

(Received 9 September 2011; revised 21 February 2012; accepted for publication 21 February 2012; published 28 March 2012)

Purpose: To establish an organ dose database for pediatric and adolescent reference individuals undergoing computed tomography (CT) examinations by using Monte Carlo simulation. The data will permit rapid estimates of organ and effective doses for patients of different age, gender, examination type, and CT scanner model.
Methods: The Monte Carlo simulation model of a Siemens Sensation 16 CT scanner previously published was employed as a base CT scanner model. A set of absorbed doses for 33 organs/tissues normalized to the product of 100 mAs and $CTDI_{vol}$ (mGy/100 mAs mGy) was established by coupling the CT scanner model with age-dependent reference pediatric hybrid phantoms. A series of single axial scans from the top of head to the feet of the phantoms was performed at a slice thickness of 10 mm, and at tube potentials of 80, 100, and 120 kVp. Using the established $CTDI_{vol}$− and 100 mAs-normalized dose matrix, organ doses for different pediatric phantoms undergoing head, chest, abdomen-pelvis, and chest-abdomen-pelvis (CAP) scans with the Siemens Sensation 16 scanner were estimated and analyzed. The results were then compared with the values obtained from three independent published methods: CT-Expo software, organ dose for abdominal CT scan derived empirically from patient abdominal circumference, and effective dose per dose-length product (DLP).
Results: Organ and effective doses were calculated and normalized to 100 mAs and $CTDI_{vol}$ for different CT examinations. At the same technical setting, dose to the organs, which were entirely included in the CT beam coverage, were higher by from 40 to 80% for newborn phantoms compared to those of 15-year phantoms. An increase of tube potential from 80 to 120 kVp resulted in 2.5–2.9-fold greater brain dose for head scans. The results from this study were compared with three different published studies and/or techniques. First, organ doses were compared to those given by CT-Expo which revealed dose differences up to several-fold when organs were partially included in the scan coverage. Second, selected organ doses from our calculations agreed to within 20% of values derived from empirical formulae based upon measured patient abdominal circumference. Third, the existing DLP-to-effective dose conversion coefficients tended to be smaller than values given in the present study for all examinations except head scans.
Conclusions: A comprehensive organ/effective dose database was established to readily calculate doses for given patients undergoing different CT examinations. The comparisons of our results with the existing studies highlight that use of hybrid phantoms with realistic anatomy is important to improve the accuracy of CT organ dosimetry. The comprehensive pediatric dose data developed here are the first organ-specific pediatric CT scan database based on the realistic pediatric hybrid phantoms which are compliant with the reference data from the International Commission on Radiological Protection (ICRP). The organ dose database is being coupled with an adult organ dose database recently published as part of the development of a user-friendly computer program enabling rapid estimates of organ and effective dose doses for patients of any age, gender, examination types, and CT scanner model. © *2012 American Association of Physicists in Medicine*. [http://dx.doi.org/10.1118/1.3693052]

I. INTRODUCTION

Although computed tomography (CT) scans have provided great benefit in patient care, increased use of the CT examinations has raised concerns regarding enhanced radiation dose and associated stochastic cancer risk to patients.[1–3] Pediatric patients are more susceptible to radiation-induced risks than are adult patients owing to their more rapidly growing tissues, their wider and increased cellular distribution of skeletal active marrow, and their greater postexposure life expectancy.

Several strategies have been introduced to reduce radiation dose to pediatric patients including pediatric scan protocols recommended by the Image Gently campaign.[4] Recently, the U.S. Food and Drug Administration (FDA) announced an "Initiative to Reduce Unnecessary Radiation Exposure from Medical Imaging" focusing on informed decision making regarding the use of CT and increasing patient awareness of their radiation dose.[5] In order to make informed decisions, a better understanding of the nature and magnitude of the organ absorbed doses resulting from CT examinations is needed, along with clinically manageable computational tools to report these organ doses.

To estimate organ doses in the human body exposed to CT x-ray photons, two different approaches are possible: experimental measurement and computer simulation. With dose measurements, physical phantoms equipped with various types of dosimeters are scanned under the CT machine and then dosimeter readings provide the information on organ doses for the specific CT system and examination. This process, however, is laborious and time-consuming and the point dose measurements cannot, in some cases, accurately represent the average organ dose when high dose gradients exist or distributed body tissues (e.g., active bone marrow) are of concern. Furthermore, physical phantoms provide a limited sampling of the variations of age, gender, and body morphometries seen in actual patient populations. Compared to physical measurement, the computer simulation approach to dose estimation has been reported to be the most sophisticated and reliable way to obtain accurate values of organ dose under CT imaging. The patient body lying on a CT scanner table and helical fan beam x-rays generated from the CT scanner are simulated in full detail under the computer simulation using 3D Monte Carlo radiation transport techniques.

The availability of computational human phantoms is a crucial part within the computer simulations which are coupled with well-established Monte Carlo transport codes. Therefore, previous studies on computer simulations of pediatric CT doses have been limited to their present availability of pediatric anatomic models. Cristy and Eckerman introduced a series of pediatric stylized phantoms where organs and body contour are described by mathematical surface equations.[6] Khurseed *et al*. utilized the Oak Ridge National Laboratory (ORNL) phantom series to estimate effective dose in CT examinations for three different CT machines.[7] However, the mathematical equations defining organ boundaries in stylized phantoms inherently have limitations in describing true human anatomy. Arm-raised positions which are normally found in clinical practice are not properly simulated and it is difficult to define scan ranges based on appropriate anatomical landmark within stylized phantoms. To overcome these anatomical limitations, more realistic computational phantoms, called voxel (or tomographic) phantoms, were reported by several authors. Zankl *et al*. developed BABY and CHILD voxel phantoms from the CT images of 8-week-old and 7-year-old baby and child, respectively, and utilized them to estimate pediatric organ doses for CT examinations.[8] Caon *et al*. developed the ADELAIDE voxel phantom based on the torso CT images of the 14-year-old female which was coupled with Monte Carlo code, EGS4, to estimate organ doses for chest and abdomen CT scans. More comprehensive pediatric voxel phantoms and their applications to CT dosimetry were reported by researchers at the University of Florida[9,10] include a newborn, 9-month male, 4-year female, 8-year female, 11-year male, and 14-year male voxel phantom series. More recently, Li *et al*. reported the organ and effective doses for 5-week female and 12-year male voxel phantoms undergoing 64-slice CT examinations.[11] Although several authors have reported organ and effective doses for pediatric patients undergoing CT examinations, the data are valid only for the specific technical conditions considered in these studies and are thus not readily expanded to different scanning protocols (e.g., scan range, tube potential, current-time-product). The software CT-Expo is the only existing general purpose dosimetry tool for pediatric patients undergoing CT examinations.[12] However, the pediatric organ dose database within this code was established considering only the BABY (8-week-old) and CHILD (7-year-old) voxel phantoms as developed in the late 1980s.

In the present study, we present a more up-to-date database of pediatric organ doses from CT examinations which are designed to rapidly provide organ doses for patients with different age, gender, examination type, and CT technical settings. These doses were derived from Monte Carlo radiation transport simulation using a series of pediatric hybrid computational phantoms with higher age resolution than the two-age phantom series found in existing software tool. The resulting organ and effective doses were compared with the values estimated by several different and published methods.

II. MATERIALS AND METHODS

II.A. CT scanner simulation

A SOMATOM Sensation 16 helical multislice CT scanner (Siemens Medical Solutions, Erlangen, Germany) was simulated within the general purpose Monte Carlo radiation transport code, MCNPX2.6.[13] Detailed technical specifications were obtained from manufacturer and simulated within MCNPX2.6 to generate unique fan-shaped x-ray beams. Instead of explicit modeling of the external bowtie filter, an angular biasing technique based on lateral free-in-air dose profile measurements was employed. To validate the simulated CT beams, a set of computed tomography dose index $(CTDI)_{100}$ data was simulated for head and body CTDI phantoms with diameters of 16 and 32 cm, respectively, and compared with the measurements. Agreement between these data was shown to be within 8.6%. Detailed descriptions of the modeling and validation work can be found in our previous publication.[14] Since MCNPX provides absorbed dose per simulated photon, the normalization factors (photons per unit mAs) were calculated based on the ratio of the ion chamber measurements free-in-air (mGy/mAs) to the simulated ion chamber doses free-in-air (mGy/photon) for head and body filters and at tube potentials of 80, 100, and 120 kVp under a collimation width of 10 mm. More detailed

explanation regarding the normalization factors is given in previous publications.[9,15]

II.B. Reference pediatric male and female hybrid phantoms

A series of reference pediatric hybrid phantoms were employed in this work: newborn, 1-year, 5-year, 10-year, and 15-year male and female phantoms developed at the University of Florida and the National Cancer Institute.[16–18] The phantoms were originally segmented from the real patient CT images of head and torso at the given ages. Arms and legs were separately segmented from high resolution CT images of arms and legs of the 18-year-old male, and then scaled to match the standard dimensions of phantoms at each respective age. A total of four reference datasets were incorporated into the final phantom series. First, the masses of organs and tissues are matched to the values in International Commission on Radiological Protection (ICRP) Publication 89.[19] Second, the reference elemental compositions for organs and tissues provided by International Commission on Radiation Units and Measurements (ICRU) Report 46 (Ref. 20) and ICRP Publication 89 were used in the Monte Carlo simulations. Third, the body dimensions are matched to the reference anthropometric data of the United States.[30] Finally, the dimensions of the alimentary tracts were matched to data given in ICRP Publication 100.[21] The pediatric hybrid phantoms include more than 40 organs as well as 35 different skeletal sites. The skeleton is composed of cortical and spongiosa structures to facilitate detailed dose calculations for both active and shallow marrow. The male and female phantoms from newborn to 10-year-old share the same anatomy except gender-specific organs such as prostate, uterus, testes, and ovaries. The 15-year-old male and female phantoms are based on totally different individuals to accurately represent their gender-specific anatomy and unique heights and weights.

Arms were removed from each pediatric phantom to more realistically simulate the typical arm-raised position in both head and torso CT scans, with the exception of the left and right humeral heads which were included to facilitate active marrow dose assessment. The original format of the phantoms was nonuniform rational B-spline (NURBS) and polygon mesh (PM) which cannot, at the present time, be directly imported into MCNPX for radiation transport. The phantoms were thus voxelized at a resolution of $2 \times 2 \times 2$ mm^3 for the newborn and 1-year phantoms and $3 \times 3 \times 3$ mm^3 for the 5-year, 10-year, and 15-year phantoms. The higher resolution was used for the two younger ages to ensure that the presence of cortical bone layer within the skeleton model was appropriately modeled in the resulting voxel format. Frontal 3D renderings of the pediatric hybrid phantoms in NURBS/PM format are shown in Fig. 1. Table I summarizes the technical parameters as well as body dimensions of the pediatric phantoms.

II.C. Organ dose matrix normalized by 100 mAs and $CTDI_{vol}$

In this study, organ doses from axial and helical scans with a given scan range were approximated as the sum of doses from multiple axial slices included in the scan range of interest; this is the same approach adopted within existing CT organ dose estimation programs.[12] The method provides great flexibility to the CT dosimetrist in which one can readily estimate organ doses for any particular CT scan coverage by using the precalculated organ dose matrix, defined as the organ doses normalized by $CTDI_{vol}$ and 100 mAs (units of mGy/100 mAs mGy per 10 mm slice), without the need to run Monte Carlo calculations for each patient case. The following equation explains one calculates scanner-specific organ doses (mGy) using the organ dose matrix and user input (SS, SE, v, $CTDI_{vol}(v)$, t, and I).

$$D(mGy) = \frac{\sum_{z=SS}^{z=SE} D(organ, age, sex, v, z)}{CTDI_{vol,Siemens}(v)} \times CTDI_{vol}(v) \cdot \left(\frac{t \cdot I}{100}\right), \quad (1)$$

where D (organ, age, sex, v, z) is the organ dose per 10 mm axial slice at longitudinal position z on the phantom and normalized to a fixed integrated tube current of 100 mAs; v is the tube potential (kVp) of the particular CT scan; z is the slice number ranging from the top of the head to the bottom of the patient's feet; SS designates the slice number where scan starts; SE designates the slice number where scan ends; $CTDI_{vol,Siemens}$ (v) is the $CTDI_{vol}$ (mGy) measured on our reference Siemens Sensation 16 scanner at a pitch of 1 and 100 mAs/rotation; $CTDI_{vol}(v)$ is for the particular scanner for which organ doses are sought is defined as CTDIw divided by pitch at 100 mAs/rotation; and t is the single rotation time (s); and I is the tube current (mA) for that particular CT scan.

Different sets of organ dose calculations were performed for a single axial scan which started from the top of head down to the bottom of the phantom's feet with an interval of 10 mm. A total of 48 (newborn male and female), 77 (1-year male and female), 111 (5-year male and female), 140 (10-year male and female), 162 (15-year female), and 167 (15-year male) consecutive axial calculations were performed. Although the male and

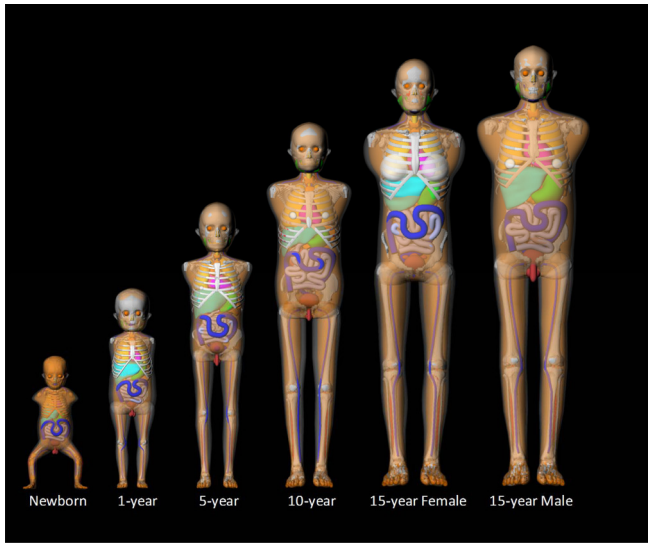

FIG. 1. 3D frontal views of the series of the pediatric hybrid phantoms representing newborn, 1, 5, 10, and 15-year-old males and females. Only male phantoms are presented from newborn to 10-year-old phantoms because the male and female share the same anatomy except gender-specific organs.

TABLE I. Voxel resolutions, array sizes, and body dimensions (height, weight, and abdominal circumference) for the newborn, 1-year, 5-year, 10-year, and 15-year male and female UF/NCI hybrid phantoms.

Parameters	Newborn M/F	1-year M/F	5-year M/F	10-year M/F	15-year F	15-year M
Voxel resolution (mm^3)	$2 \times 2 \times 2$	$2 \times 2 \times 2$	$3 \times 3 \times 3$	$3 \times 3 \times 3$	$3 \times 3 \times 3$	$3 \times 3 \times 3$
Array size	$120 \times 74 \times 242$	$97 \times 87 \times 386$	$97 \times 70 \times 372$	$114 \times 78 \times 470$	$133 \times 98 \times 541$	$147 \times 97 \times 558$
Height (cm)	48	77	111	140	162	167
Weight (kg)	3.5	10.0	18.1	32.4	53.3	56.8
Abdominal circumference (cm)	37	53	58	71	83	88

female phantoms of the newborn, 1-year, 5-year, and 10-year share the same anatomy, with the exception of gender-specific organs, two separate male and female phantoms were generated at each age and implemented into the MCNPX code for dose calculations.

To undertake dose calculations to the skeletal tissues, recently published fluence-to-dose response functions developed at the University of Florida[22] were adopted to estimate the absorbed dose to active marrow and endosteum (shallow marrow). Energy-dependent photon fluence to the spongiosa volume in a total of 34 bone sites was scored for 25 energy bins ranging from 0.01 to 10 MeV. Active marrow doses in each bone site were then calculated by multiplying the fluence-to-dose response functions for active marrow. Total absorbed doses for active marrow were calculated by weighting site-specific doses by active marrow distribution in the reference pediatric males and females.

A total of 33 organs and tissues including active marrow were involved in the organ dose calculations under tube potentials of 80, 100, and 120 kVp and the collimation width of 10 mm, resulting in approximately 4300 MCNPX input files. Kinetic energy released in matter (KERMA) approximation was assumed considering the photon energy spectra used in the simulation. Two dedicated computation servers each equipped with 8 CPUs and 16 GB RAM were employed for the Monte Carlo calculations. A total of 10^7 photons were simulated for each axial slice calculation to obtain reasonable relative errors below 1% for major organs and tissues close to the axial slice position. Data analysis was performed using an in-house postprocesser written in MATLAB language. The entire set of Monte Carlo calculations and postprocessing tasks took about 2 weeks. Finally, the five dimensional (5D) dose matrix, *Dose (age, gender, organ, slice, tube potential)*, was obtained from many sets of Monte Carlo calculations for different variables: 5 ages (newborn, 1-year, 5-year, 10-year, and 15-year), 2 genders (male and female), 33 organs, 167 slices (for 15-year-old male phantom), and 3 tube potentials (80, 100, and 120 kVp). The resulting dose matrix (mGy/100mAs) was normalized to the $CTDI_{vol}$ measurements (mGy) from the Siemens Sensation 16 CT scanner to eliminate scanner-specific characteristics. Organ doses for scanners with different x-ray tube outputs can thus be estimated through proportional scaling by machine-specific measured values of $CTDI_{vol}$.

Effective doses for different ages and tube potentials were also included in the dose matrix calculations. In ICRP Publication 103, the effective dose, E, is shown to be computed from the equivalent doses assessed for organ or tissue T of the Reference Male, H_T^M, and Reference Female, H_T^F, according to the following expression:

$$E = \sum_T W_T \left[\frac{H_T^M + H_T^F}{2}\right] \quad (2)$$

where breast and gonad doses from male and female phantoms are averaged and weighted by tissue weighting factors, w_T. Two sets of the tissue weighting factors recommended in ICRP Publication 60 and 103, respectively, were adopted in the calculations to investigate the difference in the resulting effective doses (Table II). Effective doses using the tissue weighting factors from ICRP Publication 60 and 103, ED_{60} and ED_{103}, respectively, were estimated for newborn, 1-year, 5-year, 10-year, and 15-year male and female individuals. To investigate how much higher organ doses received by pediatric patients are in comparison to those in adult patients, adult effective doses were calculated by applying the tissue weighting factors to the organ doses of the adult male and female phantoms previously published by the authors.[14]

II.D. Organ and effective doses for major scan types and specific scanner

By using the 5D dose matrix, organ doses (mGy/100 mAs mGy) were calculated by summation of organ doses

TABLE II. Tissue weighting factors published in ICRP Publications 60 and 103.

Organ or tissue	ICRP60	ICRP103
Gonads	0.2	0.08
Red bone marrow	0.12	0.12
Lung	0.12	0.12
Colon	0.12	0.12
Stomach	0.12	0.12
Breast	0.05	0.12
Bladder	0.05	0.04
Liver	0.05	0.04
Esophagus	0.05	0.04
Thyroid	0.05	0.04
Skin	0.01	0.01
Bone surface	0.01	0.01
Brain[a]		0.01
Salivary glands[b]		0.01
Remainder	0.05	0.12
Total	1	1

[a]Brain is included in the remainder in ICRP60.
[b]Tissue weighting factor was not given to salivary glands in ICRP60.

from multiple 10-mm axial slices as given by four major scan ranges: head, chest, abdomen–pelvis, and chest–abdomen-pelvis (CAP) examinations. Typical scan ranges for the four CT examinations were obtained from CT scan protocols utilized at the Department of Radiology at the University of Florida Shands Hospital.[31] These protocols were confirmed to be in good agreement with others available in the literature. The head examination covers from the top of the head to the 2nd cervical vertebra. The chest examination represents a scan from the clavicles to the middle of the liver. The abdomen–pelvis examination covers the anatomy ranging from the top of liver to the midfemoral head. Finally, CAP examination range from the clavicles to the midfemoral head. Each anatomical landmark was carefully identified in the pediatric phantom series and used for the selection of axial slices for organ dose summation. The absorbed doses to a total of 33 organs and tissues normalized to $CTDI_{vol}$ and 100 mAs (mGy/100 mAs mGy) were obtained for newborn, 1-year, 5-year, 10-year, and 15-year male and female phantoms at tube potentials of 80, 100, and 120 kVp.

To provide more clinically-relevant organ doses, normalized organ and effective doses were scaled by $CTDI_{vol}$ measurements made at tube potentials of 80, 100, and 120 kVp for the Siemens Sensation 16 reference scanner. $CTDI_{vol}$ values from the acrylic head CTDI phantom (6.1, 10.8, and 15.0 mGy for 80, 100, and 120 kVp, respectively) were used for pediatric head/body scans. $CTDI_{vol}$ values for the body phantom were 1.9, 3.8, and 5.7 mGy for 80, 100, and 120 kVp, respectively, for readers' information.

II.E. Comparison with other studies

Organ and effective doses for the head, chest, abdomen–pelvis, and CAP scans estimated in this study were compared with three different existing data reported by independent research groups. First, the selected organ doses from pediatric phantoms in this study at a tube potential of 120 kVp were compared with the values given by the software code, CT-Expo. Organ doses from our study and CT-Expo obtained for Siemens Sensation 16 scanner were normalized to the $CTDI_{vol}$ data obtained from our measurement and as given in CT-Expo, respectively, to eliminate effects of CT scanner-specific features such as filtration design and inherent x-ray tube output. Turner *et al.*[23] reported that the coefficients of variation across four different CT scanners from each of the four major manufacturers decreased from 34.1% to 5.2% on average when the organ doses were normalized by scanner-specific $CTDI_{vol}$ measurements. $CTDI_{vol}$ values for head phantom at the tube potential of 120 kVp, were used for the normalizations of pediatric head and body scans in our calculation (15.0 mGy) and in CT-Expo (21.3 mGy), respectively.

Second, our organ dose data are based on the age of the phantoms, not on the body size which is usually not available nor is feasible to abstract in large-scale retrospective cohort epidemiologic studies. In this case, there is no indicator to estimate the size of patients other than age. Some selected organ doses from the pediatric phantom series were compared with the organ doses derived from abdominal circumferences which is the method reported by Turner *et al.*[24] They calculated organ doses for a total of eight different patient voxel phantoms ranging from newborn to adult by using Monte Carlo simulations of four MDCT CT scanners from the four major manufacturers, and obtained an empirical formulae correlating doses for in-field organs in abdominal scan with patient perimeter as measured at the central slice of the abdominal scan region through exponential regression analysis. By comparing the organ doses derived from the formulae with organ doses from our database, we wanted to verify that the reference body size corresponding to the age of the phantoms follow this correlation. Absorbed doses for liver, stomach, adrenals, kidney, pancreas, spleen, and gall bladder were selected from our results of abdomen–pelvis scans, and then compared with the organ doses derived from the exponential regression coefficients provided in Turner *et al.*

Third, the effective doses calculated in this study were normalized to the dose-length product (DLP) and compared with the existing DLP-to-effective dose conversion coefficients, so called k-factors, which are derived by Shrimpton *et al.* in their study using stylized anatomic phantoms.[7,25]

III. RESULTS AND DISCUSSION

III.A. Organ and effective dose matrix for specific scan types

The 5D dose database (mGy/100 mAs mGy), *Dose (age, gender, organ, slice, tube potential)*, including a total of 33 organ and tissue doses and two effective doses, ED_{60} and ED_{103}, were established for ten different computational hybrid reference phantoms: newborn, 1-year, 5-year, 10-year, and 15-year males and females. The organ and effective doses were calculated at tube potentials of 80, 100, and 120 kVp and for both the head and body filters, and subsequently normalized to the product of 100 mAs and $CTDI_{vol}$. By using the 5D dose matrix, organ doses for the four major scan types were calculated as the summation of doses from multiple axial slices and tabulated in Tables III–VI for head, chest, abdomen–pelvis, and CAP scans, respectively. Since the newborn, 1-year, 5-year, and 10-year male and female phantoms have the identical anatomy with the exception of their gender-specific organs (prostate, uterus, testes, and ovaries), organ doses from only the male phantoms are presented. The absorbed doses for the gender-specific organs were obtained from separate male and female phantoms. Users can obtain scanner- and scan type-specific organ and effective doses using the values in Tables III–VI which are equivalent with $\frac{\sum_{z=SS}^{z=SE} D(organ,age,sex,v,z)}{CTDI_{vol,Siemens}(v)}$ in Eq. (1) for head, chest, abdomen–pelvis, and CAP, and one's own scan parameters: $CTDI_{vol}$, single rotation time (s), and tube current (mA). Since the doses in Tables III–VI are calculated only for 80, 100, and 120 kVp, it is recommended to interpolate or extrapolate the doses if users have tube potential other than those values.

III.B. Scanner-specific organ and effective doses

To provide and analyze more clinically-relevant organ doses, those specific to Siemens Sensation 16 scanner and

TABLE III. $CTDI_{vol}$– and 100 mAs-normalized organ absorbed doses (mGy/100 mAs mGy) and effective doses (mSv/100 mAs mGy) based on tissue weighting factors from either ICRP 60 (ED_{60}) or ICRP 103 (E_{103}) for the newborn, 1-year, 5-year, 10-year, and 15-year male and female reference phantoms for **head examinations** at tube potentials of 80, 100, and 120 kVp.

Head scan	Newborn[a]			1-year[a]			5-year[a]			10-year[a]			15-year female			15-year-male		
Tube potential (kVp)	80 kVp	100 kVp	120 kVp	80 kVp	100 kVp	120 kVp	80 kVp	100 kVp	120 kVp	80 kVp	100 kVp	120 kVp	80 kVp	100 kVp	120 kVp	80 kVp	100 kVp	120 kVp
Brain	1.021	1.025	1.051	0.818	0.861	0.925	0.713	0.773	0.854	0.689	0.751	0.834	0.656	0.722	0.808	0.619	0.685	0.772
Pituitary gland	0.866	0.906	0.978	0.627	0.711	0.811	0.632	0.702	0.788	0.600	0.672	0.766	0.589	0.672	0.780	0.498	0.601	0.707
Lens	1.107	1.069	1.063	0.976	0.952	0.943	0.931	0.922	0.919	0.892	0.884	0.888	1.000	0.990	0.990	0.948	0.933	0.936
Eye balls	1.026	1.019	1.028	0.985	0.983	0.989	0.885	0.897	0.924	0.852	0.869	0.900	0.893	0.906	0.934	0.887	0.895	0.921
Salivary glands	0.536	0.548	0.572	0.436	0.460	0.498	0.694	0.726	0.775	0.611	0.639	0.683	0.679	0.714	0.768	0.696	0.735	0.795
Oral cavity	0.363	0.378	0.402	0.658	0.706	0.777	0.623	0.685	0.777	0.583	0.646	0.727	0.432	0.486	0.555	0.420	0.471	0.540
Spinal cord	0.044	0.047	0.050	0.053	0.057	0.062	0.059	0.065	0.072	0.027	0.029	0.032	0.103	0.114	0.128	0.116	0.128	0.145
Thyroid	0.161	0.167	0.175	0.098	0.108	0.122	0.080	0.092	0.107	0.064	0.074	0.085	0.041	0.048	0.057	0.036	0.043	0.051
Esophagus	0.042	0.048	0.052	0.068	0.075	0.087	0.040	0.045	0.054	0.022	0.027	0.032	0.011	0.014	0.018	0.012	0.015	0.019
Trachea	0.060	0.067	0.074	0.089	0.097	0.112	0.049	0.059	0.068	0.033	0.041	0.047	0.018	0.022	0.027	0.020	0.024	0.031
Thymus	0.049	0.053	0.058	0.042	0.047	0.054	0.027	0.032	0.038	0.019	0.023	0.028	0.017	0.020	0.024	0.012	0.016	0.020
Lungs	0.033	0.035	0.039	0.026	0.029	0.034	0.024	0.027	0.032	0.011	0.013	0.017	0.008	0.010	0.012	0.007	0.008	0.010
Breast	0.016	0.015	0.021	0.011	0.012	0.013	0.006	0.008	0.009	0.004	0.004	0.005	0.002	0.003	0.003	0.002	0.002	0.002
Heart wall	0.028	0.030	0.033	0.020	0.022	0.026	0.012	0.014	0.017	0.006	0.008	0.010	0.004	0.005	0.007	0.003	0.004	0.005
Stomach wall	0.008	0.009	0.011	0.006	0.007	0.009	0.004	0.004	0.005	0.001	0.002	0.002	0.001	0.001	0.001	0.001	0.001	0.001
Liver	0.013	0.014	0.015	0.007	0.008	0.010	0.004	0.005	0.006	0.002	0.002	0.003	0.001	0.001	0.002	0.001	0.001	0.001
Gall bladder	0.006	0.007	0.007	0.003	0.004	0.006	0.002	0.002	0.003	0.001	0.001	0.002	0.000	0.001	0.001	0.000	0.000	0.001
Adrenals	0.010	0.011	0.012	0.009	0.010	0.012	0.004	0.005	0.006	0.002	0.002	0.003	0.001	0.001	0.001	0.001	0.001	0.001
Spleen	0.012	0.013	0.015	0.008	0.010	0.012	0.004	0.005	0.006	0.002	0.003	0.003	0.001	0.001	0.002	0.001	0.001	0.001
Pancreas	0.007	0.008	0.010	0.003	0.004	0.005	0.002	0.002	0.003	0.001	0.001	0.001	0.000	0.001	0.001	0.000	0.000	0.001
Kidney	0.007	0.007	0.008	0.005	0.006	0.007	0.002	0.003	0.004	0.001	0.001	0.002	0.001	0.001	0.001	0.000	0.001	0.001
Small intestine wall	0.003	0.004	0.005	0.001	0.002	0.002	0.001	0.001	0.001	0.000	0.000	0.000	0.000	0.000	0.000	0.000	0.000	0.000
Colon wall	0.005	0.005	0.006	0.002	0.002	0.002	0.001	0.001	0.001	0.000	0.000	0.001	0.000	0.000	0.000	0.000	0.000	0.000
Rectosigmoid wall	0.002	0.003	0.004	0.001	0.001	0.001	0.000	0.000	0.001	0.000	0.000	0.000	0.000	0.000	0.000	0.000	0.000	0.000
Urinary bladder wall	0.001	0.001	0.002	0.000	0.001	0.001	0.000	0.000	0.000	0.000	0.000	0.000	0.000	0.000	0.000	0.000	0.000	0.000
Prostate[b]	0.000	0.000	0.001	0.000	0.000	0.001	0.000	0.000	0.000	0.000	0.000	0.000	NA[d]	NA	NA	0.000	0.000	0.000
Uterus[b]	0.001	0.001	0.002	0.001	0.001	0.001	0.000	0.000	0.001	0.000	0.000	0.000	0.000	0.000	0.000	NA	NA	NA
Testes[b]	0.001	0.001	0.001	0.001	0.001	0.001	0.000	0.000	0.000	0.000	0.000	0.000	NA	NA	NA	0.000	0.000	0.000
Ovaries[b]	0.002	0.002	0.002	0.000	0.001	0.001	0.000	0.000	0.000	0.000	0.000	0.000	0.000	0.000	0.000	NA	NA	NA
Skin	0.233	0.227	0.223	0.197	0.195	0.195	0.139	0.139	0.140	0.095	0.094	0.095	0.075	0.074	0.075	0.068	0.068	0.069
Muscle	0.053	0.054	0.055	0.027	0.029	0.032	0.012	0.013	0.015	0.014	0.015	0.016	0.013	0.014	0.015	0.011	0.012	0.013
Active marrow	0.262	0.282	0.314	0.295	0.325	0.368	0.235	0.266	0.312	0.126	0.144	0.169	0.075	0.086	0.103	0.084	0.097	0.116
Shallow marrow	0.427	0.455	0.498	0.237	0.262	0.296	0.215	0.243	0.280	0.136	0.154	0.179	0.104	0.119	0.138	0.108	0.124	0.144
ED_{60}[c]	0.081	0.085	0.092	0.074	0.081	0.090	0.060	0.067	0.077	0.041	0.046	0.053	0.031	0.035	0.041			
ED_{103}[c]	0.075	0.079	0.086	0.072	0.079	0.088	0.061	0.068	0.078	0.042	0.047	0.053	0.032	0.036	0.041			

[a]Gender-independent organ doses for newborn, 1-year, 5-year, and 10-year phantoms were tabulated from male phantom since male and female phantoms have identical anatomy except gender-specific organs.
[b]Gender-specific organ doses were calculated separately from male and female phantoms.
[c]Effective doses were calculated using male and female organ doses as recommended by ICRP. Effective dose for 15-year phantoms was tabulated in 15-year female columns.
[d]Male organ doses are not available (NA) for 15-year female phantom. Female organ doses are not available for 15-year male phantom.

TABLE IV. $CTDI_{vol}$– and 100 mAs-normalized organ absorbed doses (mGy/100 mAs mGy) and effective doses (mSv/100 mAs mGy) based on tissue weighting factors from either ICRP 60 (ED_{60}) or ICRP 103 (E_{103}) for the newborn, 1-year, 5-year, 10-year, and 15-year male and female reference phantoms for **chest examinations** at tube potentials of 80, 100, and 120 kVp.

Chest scan	Newborn[a]			1-year[a]			5-year[a]			10-year[a]			15-year female			15-year-male		
Tube potential (kVp)	80 kVp	100 kVp	120 kVp	80 kVp	100 kVp	120 kVp	80 kVp	100 kVp	120 kVp	80 kVp	100 kVp	120 kVp	80 kVp	100 kVp	120 kVp	80 kVp	100 kVp	120 kVp
Brain	0.039	0.043	0.047	0.020	0.024	0.028	0.014	0.017	0.021	0.014	0.018	0.022	0.008	0.011	0.014	0.007	0.009	0.012
Pituitary gland	0.038	0.041	0.053	0.020	0.025	0.031	0.010	0.014	0.014	0.010	0.013	0.017	0.007	0.009	0.011	0.004	0.007	0.009
Lens	0.038	0.044	0.048	0.013	0.017	0.021	0.008	0.010	0.012	0.008	0.010	0.014	0.005	0.007	0.009	0.009	0.010	0.013
Eye balls	0.044	0.047	0.053	0.015	0.018	0.022	0.009	0.011	0.013	0.009	0.011	0.014	0.006	0.007	0.009	0.007	0.008	0.010
Salivary glands	0.676	0.677	0.693	0.135	0.142	0.152	0.075	0.082	0.090	0.072	0.080	0.090	0.040	0.046	0.053	0.033	0.039	0.046
Oral cavity	0.307	0.313	0.327	0.082	0.089	0.098	0.048	0.054	0.063	0.043	0.050	0.058	0.043	0.050	0.058	0.034	0.040	0.047
Spinal cord	0.733	0.742	0.777	0.499	0.519	0.551	0.382	0.414	0.462	0.162	0.181	0.206	0.235	0.270	0.316	0.154	0.178	0.208
Thyroid	1.190	1.177	1.193	1.000	1.003	1.034	1.000	0.991	0.991	0.783	0.778	0.786	0.574	0.585	0.605	0.515	0.531	0.556
Esophagus	0.922	0.947	0.997	0.751	0.787	0.845	0.643	0.685	0.751	0.518	0.572	0.654	0.426	0.482	0.555	0.395	0.451	0.524
Trachea	0.961	0.985	1.024	0.882	0.898	0.954	0.826	0.851	0.906	0.606	0.651	0.724	0.540	0.594	0.667	0.493	0.542	0.615
Thymus	1.019	1.023	1.052	0.909	0.935	0.989	0.891	0.915	0.959	0.668	0.720	0.795	0.593	0.645	0.717	0.526	0.582	0.663
Lungs	1.085	1.088	1.113	1.016	1.026	1.054	0.870	0.896	0.937	0.738	0.778	0.834	0.601	0.645	0.706	0.574	0.621	0.684
Breast	1.091	1.054	1.057	0.825	0.836	0.858	0.751	0.759	0.789	0.656	0.673	0.697	0.587	0.605	0.634	0.572	0.593	0.624
Heart wall	1.128	1.130	1.154	1.004	1.023	1.065	0.886	0.918	0.965	0.741	0.789	0.859	0.643	0.692	0.759	0.615	0.672	0.747
Stomach wall	0.822	0.834	0.862	0.477	0.497	0.529	0.344	0.366	0.396	0.233	0.257	0.290	0.307	0.332	0.365	0.204	0.227	0.258
Liver	0.952	0.956	0.980	0.604	0.624	0.653	0.443	0.469	0.502	0.400	0.432	0.473	0.407	0.441	0.486	0.305	0.337	0.378
Gall bladder	0.774	0.787	0.819	0.204	0.222	0.248	0.105	0.120	0.138	0.113	0.131	0.154	0.174	0.202	0.236	0.111	0.133	0.161
Adrenals	0.828	0.845	0.887	0.716	0.746	0.793	0.393	0.423	0.466	0.228	0.254	0.289	0.235	0.271	0.314	0.198	0.232	0.270
Spleen	1.041	1.034	1.052	0.818	0.825	0.846	0.441	0.460	0.486	0.300	0.319	0.345	0.397	0.417	0.447	0.254	0.275	0.303
Pancreas	0.643	0.651	0.672	0.135	0.148	0.165	0.088	0.101	0.119	0.086	0.103	0.123	0.084	0.100	0.123	0.060	0.073	0.091
Kidney	0.301	0.304	0.315	0.253	0.270	0.293	0.105	0.119	0.138	0.075	0.088	0.105	0.073	0.087	0.105	0.060	0.074	0.091
Small intestine wall	0.142	0.149	0.158	0.047	0.053	0.061	0.020	0.025	0.030	0.017	0.022	0.028	0.021	0.026	0.033	0.013	0.017	0.023
Colon wall	0.317	0.320	0.326	0.052	0.059	0.067	0.022	0.026	0.031	0.018	0.022	0.028	0.014	0.017	0.021	0.011	0.015	0.019
Rectosigmoid wall	0.053	0.058	0.064	0.011	0.014	0.018	0.005	0.007	0.009	0.002	0.003	0.004	0.002	0.003	0.004	0.001	0.002	0.002
Urinary bladder wall	0.030	0.033	0.037	0.011	0.013	0.016	0.003	0.004	0.006	0.001	0.002	0.002	0.001	0.001	0.002	0.001	0.001	0.002
Prostate[b]	0.023	0.023	0.024	0.005	0.006	0.008	0.002	0.002	0.003	0.000	0.001	0.001	NA[d]	NA	NA	0.000	0.000	0.001
Uterus[b]	0.037	0.040	0.043	0.011	0.014	0.016	0.004	0.006	0.007	0.001	0.002	0.003	0.001	0.001	0.002	NA	NA	NA
Testes[b]	0.011	0.011	0.013	0.003	0.003	0.005	0.001	0.001	0.002	0.000	0.000	0.000	NA	NA	NA	0.000	0.000	0.001
Ovaries[b]	0.055	0.060	0.067	0.013	0.017	0.021	0.005	0.006	0.009	0.002	0.002	0.003	0.001	0.002	0.002	NA	NA	NA
Skin	0.392	0.380	0.372	0.250	0.245	0.242	0.185	0.183	0.182	0.161	0.161	0.161	0.142	0.141	0.141	0.143	0.143	0.144
Muscle	0.436	0.434	0.438	0.249	0.258	0.274	0.190	0.199	0.212	0.119	0.125	0.133	0.145	0.154	0.166	0.121	0.127	0.135
Active marrow	0.370	0.394	0.434	0.288	0.313	0.349	0.149	0.168	0.197	0.148	0.170	0.203	0.126	0.148	0.179	0.122	0.144	0.175
Shallow marrow	0.411	0.434	0.470	0.374	0.402	0.442	0.252	0.277	0.311	0.182	0.206	0.238	0.129	0.148	0.174	0.113	0.131	0.153
ED_{60}[c]	0.557	0.562	0.580	0.403	0.415	0.437	0.323	0.336	0.357	0.265	0.282	0.307	0.222	0.246	0.272			
ED_{103}[c]	0.640	0.643	0.661	0.459	0.472	0.496	0.372	0.386	0.409	0.307	0.326	0.352	0.262	0.282	0.310			

[a]Gender-independent organ doses for newborn, 1-year, 5-year, and 10-year phantoms were tabulated from male phantom since male and female phantoms have identical anatomy except gender-specific organs.
[b]Gender-specific organ doses were calculated separately from male and female phantoms.
[c]Effective doses were calculated using male and female organ doses as recommended by ICRP. Effective dose for 15-year phantoms was tabulated in 15-year female columns.
[d]Male organ doses are not available (NA) for 15-year female phantom. Female organ doses are not available for 15-year male phantom.

TABLE V. $CTDI_{vol}$– and 100 mAs-normalized organ absorbed doses (mGy/100 mAs mGy) and effective doses (mSv/100 mAs mGy) based on tissue weighting factors from either ICRP 60 (ED_{60}) or ICRP 103 (E_{103}) for the newborn, 1-year, 5-year, 10-year, and 15-year male and female reference phantoms for **abdomen-pelvis examinations** at tube potentials of 80, 100, and 120 kVp.

Abdomen-pelvis scan	Newborn[a]			1-year[a]			5-year[a]			10-year[a]			15-year female			15-year-male		
Tube potential (kVp)	80 kVp	100 kVp	120 kVp	80 kVp	100 kVp	120 kVp	80 kVp	100 kVp	120 kVp	80 kVp	100 kVp	120 kVp	20 kVp	80 kVp	120 kVp	80 kVp	100 kVp	120 kVp
Brain	0.012	0.014	0.016	0.004	0.005	0.007	0.003	0.004	0.005	0.001	0.002	0.002	0.001	0.001	0.002	0.001	0.001	0.001
Pituitary gland	0.008	0.009	0.015	0.004	0.005	0.006	0.001	0.002	0.003	0.001	0.002	0.002	0.001	0.001	0.001	0.000	0.000	0.001
Lens	0.014	0.016	0.015	0.005	0.007	0.008	0.003	0.004	0.004	0.001	0.002	0.002	0.001	0.001	0.001	0.003	0.003	0.003
Eye balls	0.014	0.016	0.017	0.004	0.005	0.007	0.002	0.003	0.004	0.001	0.001	0.002	0.001	0.001	0.001	0.001	0.001	0.001
Salivary glands	0.052	0.058	0.065	0.019	0.021	0.026	0.009	0.011	0.013	0.004	0.005	0.007	0.003	0.003	0.004	0.002	0.002	0.003
Oral cavity	0.035	0.040	0.045	0.015	0.017	0.020	0.007	0.009	0.011	0.003	0.004	0.006	0.003	0.004	0.005	0.001	0.002	0.003
Spinal cord	0.659	0.664	0.700	0.511	0.536	0.576	0.404	0.443	0.499	0.303	0.337	0.383	0.185	0.213	0.251	0.227	0.257	0.293
Thyroid	0.066	0.073	0.083	0.056	0.060	0.069	0.025	0.030	0.035	0.011	0.014	0.018	0.009	0.011	0.015	0.006	0.009	0.012
Esophagus	0.471	0.488	0.516	0.208	0.223	0.248	0.218	0.241	0.272	0.155	0.177	0.209	0.146	0.171	0.200	0.121	0.141	0.168
Trachea	0.118	0.130	0.135	0.052	0.059	0.067	0.044	0.050	0.057	0.026	0.031	0.039	0.020	0.026	0.033	0.013	0.017	0.024
Thymus	0.144	0.152	0.164	0.102	0.111	0.126	0.068	0.078	0.089	0.036	0.044	0.053	0.018	0.024	0.031	0.017	0.021	0.029
Lungs	0.626	0.630	0.646	0.468	0.479	0.496	0.276	0.289	0.308	0.236	0.251	0.272	0.158	0.175	0.196	0.172	0.190	0.212
Breast	1.007	0.978	0.983	0.773	0.785	0.807	0.732	0.739	0.768	0.284	0.296	0.310	0.343	0.356	0.375	0.484	0.502	0.529
Heart wall	0.706	0.710	0.732	0.498	0.514	0.543	0.487	0.511	0.546	0.286	0.311	0.345	0.192	0.214	0.242	0.180	0.202	0.230
Stomach wall	1.081	1.096	1.134	0.873	0.910	0.969	0.820	0.860	0.919	0.696	0.749	0.824	0.657	0.706	0.772	0.533	0.589	0.662
Liver	1.113	1.117	1.143	0.933	0.962	1.005	0.822	0.864	0.921	0.694	0.741	0.805	0.644	0.695	0.760	0.559	0.616	0.687
Gall bladder	1.006	1.025	1.069	0.849	0.901	0.976	0.771	0.838	0.912	0.668	0.730	0.814	0.536	0.607	0.702	0.458	0.530	0.621
Adrenals	0.963	0.984	1.032	0.776	0.811	0.871	0.692	0.744	0.814	0.567	0.622	0.699	0.482	0.548	0.632	0.431	0.494	0.575
Spleen	1.114	1.112	1.133	0.983	0.993	1.021	0.844	0.876	0.917	0.764	0.796	0.844	0.691	0.719	0.763	0.593	0.629	0.680
Pancreas	1.088	1.098	1.134	0.897	0.934	0.999	0.790	0.845	0.927	0.611	0.683	0.779	0.547	0.619	0.711	0.421	0.489	0.577
Kidney	1.123	1.129	1.162	1.008	1.054	1.121	0.902	0.967	1.052	0.776	0.838	0.922	0.699	0.761	0.843	0.549	0.620	0.707
Small intestine wall	1.101	1.109	1.137	0.889	0.931	0.992	0.854	0.901	0.969	0.690	0.753	0.839	0.634	0.696	0.777	0.464	0.533	0.620
Colon wall	1.170	1.158	1.164	0.971	0.998	1.039	0.965	0.986	1.024	0.832	0.866	0.918	0.828	0.855	0.894	0.590	0.644	0.715
Rectosigmoid wall	0.943	0.962	1.010	0.701	0.745	0.813	0.607	0.656	0.725	0.504	0.564	0.646	0.399	0.458	0.534	0.336	0.380	0.439
Urinary bladder wall	1.053	1.045	1.045	0.809	0.847	0.910	0.732	0.758	0.797	0.543	0.590	0.655	0.348	0.390	0.448	0.278	0.322	0.377
Prostate[b]	0.665	0.670	0.691	0.455	0.473	0.515	0.146	0.165	0.189	0.126	0.155	0.181	NA[d]	NA	NA	0.060	0.074	0.094
Uterus[b]	0.893	0.917	0.955	0.677	0.725	0.803	0.591	0.652	0.737	0.474	0.542	0.634	0.336	0.396	0.475	NA	NA	NA
Testes[b]	0.142	0.144	0.155	0.166	0.171	0.182	0.094	0.105	0.119	0.056	0.067	0.082	NA	NA	NA	0.054	0.066	0.082
Ovaries[b]	0.933	0.960	0.996	0.833	0.873	0.943	0.726	0.770	0.851	0.554	0.622	0.719	0.439	0.502	0.586	NA	NA	NA
Skin	0.497	0.482	0.470	0.377	0.370	0.366	0.290	0.287	0.286	0.254	0.253	0.253	0.211	0.210	0.210	0.202	0.202	0.202
Muscle	0.723	0.720	0.728	0.434	0.451	0.477	0.325	0.339	0.360	0.223	0.234	0.251	0.228	0.240	0.258	0.215	0.226	0.242
Active marrow	0.300	0.323	0.359	0.278	0.308	0.352	0.168	0.194	0.233	0.198	0.232	0.282	0.210	0.253	0.312	0.170	0.205	0.254
Shallow marrow	0.328	0.349	0.382	0.377	0.415	0.467	0.260	0.295	0.341	0.217	0.251	0.297	0.187	0.220	0.263	0.139	0.164	0.198
ED_{60}[c]	0.715	0.722	0.744	0.594	0.618	0.657	0.502	0.527	0.577	0.403	0.436	0.493	0.345	0.376	0.421			
ED_{103}[c]	0.737	0.740	0.760	0.590	0.613	0.649	0.514	0.538	0.574	0.395	0.425	0.467	0.348	0.380	0.422			

[a]Gender-independent organ doses for newborn, 1-year, 5-year, and 10-year phantoms were tabulated from male phantom since male and female phantoms have identical anatomy except gender-specific organs.
[b]Gender-specific organ doses were calculated separately from male and female phantoms.
[c]Effective doses were calculated using male and female organ doses as recommended by ICRP. Effective dose for 15-year phantoms was tabulated in 15-year female columns.
[d]Male organ doses are not available (NA) for 15-year female phantom. Female organ doses are not available for 15-year male phantom.

TABLE VI. $CTDI_{vol}$– and 100 mAs-normalized organ absorbed doses (mGy/100 mAs mGy) and effective doses (mSv/100 mAs mGy) based on tissue weighting factors from either ICRP 60 (ED_{60}) or ICRP 103 (E_{103}) for the newborn, 1-year, 5-year, 10-year, and 15-year male and female reference phantoms for **chest-abdomen-pelvis (CAP)** examinations at tube potentials of 80, 100, and 120 kVp.

CAP scan	Newborn[a]			1-year[a]			5-year[a]			10-year[a]			15-year female			15-year-male		
Tube potential (kVp)	80 kVp	100 kVp	120 kVp	80 kVp	100 kVp	120 kVp	80 kVp	100 kVp	120 kVp	80 kVp	100 kVp	120 kVp	80 kVp	100 kVp	120 kVp	80 kVp	100 kVp	120 kVp
Brain	0.042	0.046	0.051	0.022	0.025	0.030	0.015	0.019	0.023	0.015	0.018	0.023	0.009	0.011	0.014	0.007	0.009	0.012
Pituitary gland	0.041	0.044	0.056	0.022	0.027	0.032	0.010	0.015	0.016	0.011	0.013	0.018	0.007	0.009	0.011	0.005	0.007	0.009
Lens	0.042	0.049	0.052	0.016	0.020	0.024	0.009	0.012	0.014	0.008	0.011	0.015	0.005	0.007	0.010	0.010	0.011	0.014
Eye balls	0.047	0.050	0.057	0.016	0.019	0.025	0.010	0.012	0.015	0.010	0.012	0.015	0.006	0.008	0.010	0.007	0.008	0.010
Salivary glands	0.685	0.688	0.704	0.140	0.148	0.160	0.078	0.085	0.095	0.073	0.082	0.093	0.041	0.047	0.054	0.034	0.040	0.047
Oral cavity	0.313	0.321	0.336	0.086	0.094	0.104	0.051	0.057	0.067	0.044	0.052	0.061	0.044	0.051	0.060	0.034	0.041	0.048
Spinal cord	1.005	1.016	1.066	0.796	0.832	0.890	0.647	0.705	0.792	0.410	0.456	0.519	0.356	0.409	0.478	0.317	0.363	0.419
Thyroid	1.201	1.190	1.207	1.012	1.019	1.054	1.007	1.000	1.001	0.786	0.782	0.792	0.576	0.587	0.609	0.516	0.533	0.559
Esophagus	0.961	0.990	1.045	0.782	0.824	0.890	0.685	0.734	0.810	0.554	0.615	0.708	0.452	0.515	0.596	0.418	0.479	0.560
Trachea	0.977	1.004	1.046	0.894	0.913	0.973	0.838	0.865	0.923	0.613	0.660	0.737	0.544	0.600	0.675	0.495	0.546	0.621
Thymus	1.036	1.044	1.076	0.930	0.960	1.019	0.906	0.933	0.981	0.677	0.732	0.810	0.597	0.650	0.724	0.529	0.586	0.669
Lungs	1.123	1.131	1.159	1.074	1.091	1.127	0.911	0.943	0.992	0.777	0.824	0.889	0.622	0.673	0.739	0.597	0.650	0.720
Breast	1.106	1.074	1.079	0.855	0.868	0.897	0.788	0.798	0.836	0.675	0.695	0.725	0.605	0.627	0.660	0.587	0.612	0.648
Heart wall	1.167	1.173	1.203	1.066	1.092	1.144	0.949	0.990	1.050	0.785	0.843	0.925	0.667	0.723	0.798	0.637	0.700	0.783
Stomach wall	1.126	1.143	1.185	0.944	0.987	1.053	0.870	0.917	0.984	0.740	0.802	0.887	0.697	0.753	0.829	0.565	0.628	0.710
Liver	1.184	1.191	1.222	1.006	1.042	1.093	0.883	0.933	0.999	0.764	0.822	0.898	0.696	0.756	0.834	0.600	0.666	0.748
Gall bladder	1.039	1.058	1.105	0.883	0.939	1.022	0.793	0.864	0.943	0.695	0.763	0.855	0.562	0.641	0.744	0.478	0.556	0.655
Adrenals	1.006	1.030	1.082	0.869	0.912	0.980	0.744	0.805	0.886	0.612	0.676	0.764	0.512	0.588	0.683	0.462	0.535	0.626
Spleen	1.176	1.176	1.202	1.063	1.078	1.114	0.902	0.941	0.990	0.812	0.852	0.909	0.729	0.764	0.818	0.625	0.667	0.727
Pancreas	1.118	1.131	1.170	0.923	0.965	1.034	0.811	0.870	0.957	0.634	0.713	0.816	0.563	0.639	0.738	0.434	0.506	0.600
Kidney	1.149	1.157	1.192	1.049	1.100	1.174	0.927	0.997	1.089	0.797	0.863	0.954	0.713	0.779	0.867	0.562	0.636	0.729
Small intestine wall	1.115	1.124	1.155	0.899	0.943	1.006	0.865	0.914	0.985	0.695	0.759	0.848	0.638	0.702	0.784	0.467	0.537	0.626
Colon wall	1.185	1.174	1.183	0.981	1.010	1.053	0.974	0.997	1.037	0.837	0.873	0.926	0.830	0.858	0.898	0.592	0.648	0.719
Rectosigmoid wall	0.951	0.970	1.019	0.704	0.749	0.817	0.659	0.711	0.786	0.505	0.565	0.648	0.400	0.459	0.535	0.336	0.381	0.440
Urinary bladder wall	1.058	1.050	1.051	0.812	0.850	0.914	0.867	0.895	0.936	0.543	0.590	0.656	0.348	0.391	0.449	0.278	0.322	0.377
Prostate[b]	0.668	0.673	0.695	0.457	0.475	0.516	0.211	0.231	0.259	0.126	0.155	0.182	NA[d]	NA	NA	0.060	0.074	0.094
Uterus[b]	0.900	0.923	0.961	0.680	0.729	0.807	0.620	0.684	0.772	0.474	0.543	0.635	0.336	0.396	0.475	NA	NA	NA
Testes[b]	0.144	0.146	0.157	0.166	0.172	0.183	0.127	0.138	0.155	0.056	0.067	0.082	NA	NA	NA	0.054	0.067	0.083
Ovaries[b]	0.940	0.967	1.005	0.837	0.879	0.949	0.755	0.804	0.888	0.554	0.622	0.721	0.439	0.503	0.587	NA	NA	NA
Skin	0.673	0.652	0.637	0.521	0.511	0.504	0.418	0.414	0.412	0.369	0.368	0.368	0.306	0.305	0.305	0.302	0.301	0.302
Muscle	0.884	0.880	0.890	0.567	0.588	0.623	0.442	0.462	0.492	0.306	0.321	0.343	0.326	0.343	0.369	0.292	0.307	0.328
Active marrow	0.505	0.542	0.600	0.455	0.500	0.567	0.283	0.325	0.386	0.308	0.360	0.435	0.302	0.361	0.443	0.259	0.310	0.383
Shallow marrow	0.558	0.592	0.644	0.620	0.676	0.754	0.461	0.517	0.590	0.362	0.415	0.485	0.285	0.332	0.394	0.225	0.264	0.314
ED_{60}[c]	0.908	0.917	0.946	0.782	0.821	0.871	0.699	0.732	0.792	0.576	0.619	0.689	0.473	0.518	0.576			
ED_{103}[c]	0.936	0.942	0.969	0.790	0.818	0.865	0.705	0.736	0.785	0.591	0.632	0.691	0.487	0.531	0.589			

[a]Gender-independent organ doses for newborn, 1-year, 5-year, and 10-year phantoms were tabulated from male phantom since male and female phantoms have identical anatomy except gender-specific organs.
[b]Gender-specific organ doses were calculated separately from male and female phantoms.
[c]Effective doses were calculated using male and female organ doses as recommended by ICRP. Effective dose for 15-year phantoms was tabulated in 15-year female columns.
[d]Male organ doses are not available (NA) for 15-year female phantom. Female organ doses are not available for 15-year male phantom.

TABLE VII. Organ absorbed doses (mGy/100 mAs) and effective doses (mSv/100 mAs) for newborn, 1-year, 5-year, 10-year, and 15-year male and female reference phantoms for **head CT examinations** using the Siemens SOMATOM Sensation 16 scanner model at tube potentials of 80, 100, and 120 kVp. The significant digits of table entries reflect the precision of the Monte Carlo calculations. Organ doses less than 0.1 mGy/100 mAs are not tabulated (indicated by a hyphen).

Head scan	Newborn[a]			1-year[a]			5-year[a]			10-year[a]			15-year female			15-year-male		
Tube potential (kVp)	80 kVp	100 kVp	120 kVp	80 kVp	100 kVp	120 kVp	80 kVp	100 kVp	120 kVp	80kVp	100 kVp	120 kVp	80 kVp	100 kVp	120 kVp	80 kVp	100 kVp	120 kVp
Brain	6.2	11.1	15.8	5.0	9.3	13.9	4.3	8.3	12.8	4.2	8.1	12.5	4.0	7.8	12.1	3.8	7.4	11.6
Pituitary gland	5.3	9.8	14.7	3.8	7.7	12.2	3.9	7.6	11.8	3.7	7.3	11.5	3.6	7.3	11.7	3.0	6.5	10.6
Lens	6.8	11.5	15.9	6.0	10.3	14.1	5.7	10.0	13.8	5.4	9.5	13.3	6.1	10.7	14.9	5.8	10.1	14.0
Eye balls	6.3	11.0	15.4	6.0	10.6	14.8	5.4	9.7	13.9	5.2	9.4	13.5	5.4	9.8	14.0	5.4	9.7	13.8
Salivary glands	3.3	5.9	8.6	2.7	5.0	7.5	4.2	7.8	11.6	3.7	6.9	10.2	4.1	7.7	11.5	4.2	7.9	11.9
Oral cavity	2.2	4.1	6.0	4.0	7.6	11.7	3.8	7.4	11.7	3.6	7.0	10.9	2.6	5.2	8.3	2.6	5.1	8.1
Spinal cord	0.3	0.5	0.8	0.3	0.6	0.9	0.4	0.7	1.1	0.2	0.3	0.5	0.6	1.2	1.9	0.7	1.4	2.2
Thyroid	1.0	1.8	2.6	0.6	1.2	1.8	0.5	1.0	1.6	0.4	0.8	1.3	0.3	0.5	0.9	0.2	0.5	0.8
Esophagus	0.3	0.5	0.8	0.4	0.8	1.3	0.2	0.5	0.8	0.1	0.3	0.5	0.1	0.2	0.3	0.1	0.2	0.3
Trachea	0.4	0.7	1.1	0.5	1.0	1.7	0.3	0.6	1.0	0.2	0.4	0.7	0.1	0.2	0.4	0.1	0.3	0.5
Thymus	0.3	0.6	0.9	0.3	0.5	0.8	0.2	0.3	0.6	0.1	0.2	0.4	0.1	0.2	0.4	0.1	0.2	0.3
Lungs	0.2	0.4	0.6	0.2	0.3	0.5	0.1	0.3	0.5	0.1	0.1	0.3	–	0.1	0.2	–	0.1	0.2
Breast	0.1	0.2	0.3	0.1	0.1	0.2	0.0	0.1	0.1	–	–	0.1	–	–	–	–	–	–
Heart wall	0.2	0.3	0.5	0.1	0.2	0.4	0.1	0.2	0.3	–	0.1	0.2	–	0.1	0.1	–	–	0.1
Stomach wall	–	0.1	0.2	–	0.1	0.1	–	–	0.1	–	–	–	–	–	–	–	–	–
Liver	0.1	0.2	0.2	–	0.1	0.2	–	0.1	0.1	–	–	–	–	–	–	–	–	–
Gall bladder	–	0.1	0.1	–	–	0.1	–	–	–	–	–	–	–	–	–	–	–	–
Adrenals	0.1	0.1	0.2	0.1	0.1	0.2	–	0.1	0.1	–	–	–	–	–	–	–	–	–
Spleen	0.1	0.1	0.2	–	0.1	0.2	–	0.1	0.1	–	–	–	–	–	–	–	–	–
Pancreas	–	0.1	0.2	–	–	0.1	–	–	–	–	–	–	–	–	–	–	–	–
Kidney	–	0.1	0.1	–	0.1	0.1	–	–	0.1	–	–	–	–	–	–	–	–	–
Small intestine wall	–	–	0.1	–	–	–	–	–	–	–	–	–	–	–	–	–	–	–
Colon wall	–	0.1	0.1	–	–	–	–	–	–	–	–	–	–	–	–	–	–	–
Rectosigmoid wall	–	–	0.1	–	–	–	–	–	–	–	–	–	–	–	–	–	–	–
Urinary bladder wall	–	–	–	–	–	–	–	–	–	–	–	–	–	–	–	–	–	–
Prostate[b]	–	–	–	–	–	–	–	–	–	–	–	–	NA[d]	NA	NA	–	–	–
Uterus[b]	–	–	–	–	–	–	–	–	–	–	–	–	–	–	–	NA	NA	NA
Testes[b]	–	–	–	–	–	–	–	–	–	–	–	–	NA	NA	NA	–	–	–
Ovaries[b]	–	–	–	–	–	–	–	–	–	–	–	–	–	–	–	NA	NA	NA
Skin	1.4	2.5	3.3	1.2	2.1	2.9	0.8	1.5	2.1	0.6	1.0	1.4	0.5	0.8	1.1	0.4	0.7	1.0
Muscle	0.3	0.6	0.8	0.2	0.3	0.5	0.1	0.1	0.2	0.1	0.2	0.2	0.1	0.2	0.2	0.1	0.1	0.2
Active marrow	1.6	3.0	4.7	1.8	3.5	5.5	1.4	2.9	4.7	0.8	1.6	2.5	0.5	0.9	1.5	0.5	1.0	1.7
Shallow marrow	2.6	4.9	7.5	1.4	2.8	4.4	1.3	2.6	4.2	0.8	1.7	2.7	0.6	1.3	2.1	0.7	1.3	2.2
ED_{60}[c]	0.5	0.9	1.4	0.5	0.9	1.4	0.4	0.7	1.2	0.3	0.5	0.8	0.2	0.4	0.6			
ED_{103}[c]	0.5	0.8	1.3	0.4	0.8	1.3	0.4	0.7	1.2	0.3	0.5	0.8	0.2	0.4	0.6			

[a]Gender-independent organ doses for newborn, 1-year, 5-year, and 10-year phantoms were tabulated from male phantom since male and female phantoms have identical anatomy except gender-specific organs.
[b]Gender-specific organ doses were calculated separatelyfrom male and female phantoms.
[c]Effective doses were calculated using male and female organ doses as recommended by ICRP. Effective dose for 15-year phantoms was tabulated in 15-year female columns.
[d]Male organ doses are not available (NA) for 15-yearfemale phantom. Female organ doses are not available for 15-year male phantom.

TABLE VIII. Organ absorbed doses (mGy/100 mAs) and effective doses (mSv/100 mAs) for newborn, 1-year, 5-year, 10-year, and 15-year male and female reference phantoms for **chest CT examinations** using the Siemens SOMATOM Sensation 16 scanner model at tube potentials of 80, 100, and 120 kVp. The significant digits of table entries reflect the precision of the Monte Carlo calculations. Organ doses less than 0.1 mGy/100 mAs are not tabulated (indicated by a hyphen).

Chest scan	Newborn[a]			1-year[a]			5-year[a]			10-year[a]			15-year female			15-year-male		
Tube potential (kVp)	80 kVp	100 kVp	120 kVp	80 kVp	100 kVp	120 kVp	80 kVp	100 kVp	120 kVp	80 kVp	100 kVp	120 kVp	80 kVp	100 kVp	120 kVp	80 kVp	100 kVp	120 kVp
Brain	0.2	0.5	0.7	0.1	0.3	0.4	0.1	0.2	0.3	0.1	0.2	0.3	–	0.1	0.2	–	0.1	0.2
Pituitary gland	0.2	0.4	0.8	0.1	0.3	0.5	0.1	0.2	0.2	0.1	0.1	0.3	–	0.1	0.2	–	0.1	0.1
Lens	0.2	0.5	0.7	0.1	0.2	0.3	–	0.1	0.2	–	0.1	0.2	–	0.1	0.1	0.1	0.1	0.2
Eye balls	0.3	0.5	0.8	0.1	0.2	0.3	0.1	0.1	0.2	0.1	0.1	0.2	–	0.1	0.1	–	0.1	0.2
Salivary glands	4.1	7.3	10.4	0.8	1.5	2.3	0.5	0.9	1.4	0.4	0.9	1.4	0.2	0.5	0.8	0.2	0.4	0.7
Oral cavity	1.9	3.4	4.9	0.5	1.0	1.5	0.3	0.6	0.9	0.3	0.5	0.9	0.3	0.5	0.9	0.2	0.4	0.7
Spinal cord	4.5	8.0	11.7	3.0	5.6	8.3	2.3	4.5	6.9	1.0	2.0	3.1	1.4	2.9	4.7	0.9	1.9	3.1
Thyroid	7.3	12.7	17.9	6.1	10.8	15.5	6.1	10.7	14.9	4.8	8.4	11.8	3.5	6.3	9.1	3.1	5.7	8.3
Esophagus	5.6	10.2	15.0	4.6	8.5	12.7	3.9	7.4	11.3	3.2	6.2	9.8	2.6	5.2	8.3	2.4	4.9	7.9
Trachea	5.9	10.6	15.4	5.4	9.7	14.3	5.0	9.2	13.6	3.7	7.0	10.9	3.3	6.4	10.0	3.0	5.9	9.2
Thymus	6.2	11.0	15.8	5.5	10.1	14.8	5.4	9.9	14.4	4.1	7.8	11.9	3.6	7.0	10.8	3.2	6.3	9.9
Lungs	6.6	11.8	16.7	6.2	11.1	15.8	5.3	9.7	14.1	4.5	8.4	12.5	3.7	7.0	10.6	3.5	6.7	10.3
Breast	6.7	11.4	15.9	5.0	9.0	12.9	4.6	8.2	11.8	4.0	7.3	10.5	3.6	6.5	9.5	3.5	6.4	9.4
Heart wall	6.9	12.2	17.3	6.1	11.0	16.0	5.4	9.9	14.5	4.5	8.5	12.9	3.9	7.5	11.4	3.8	7.3	11.2
Stomach wall	5.0	9.0	12.9	2.9	5.4	7.9	2.1	4.0	5.9	1.4	2.8	4.4	1.9	3.6	5.5	1.2	2.5	3.9
Liver	5.8	10.3	14.7	3.7	6.7	9.8	2.7	5.1	7.5	2.4	4.7	7.1	2.5	4.8	7.3	1.9	3.6	5.7
Gall bladder	4.7	8.5	12.3	1.2	2.4	3.7	0.6	1.3	2.1	0.7	1.4	2.3	1.1	2.2	3.5	0.7	1.4	2.4
Adrenals	5.1	9.1	13.3	4.4	8.1	11.9	2.4	4.6	7.0	1.4	2.7	4.3	1.4	2.9	4.7	1.2	2.5	4.1
Spleen	6.4	11.2	15.8	5.0	8.9	12.7	2.7	5.0	7.3	1.8	3.4	5.2	2.4	4.5	6.7	1.5	3.0	4.5
Pancreas	3.9	7.0	10.1	0.8	1.6	2.5	0.5	1.1	1.8	0.5	1.1	1.8	0.5	1.1	1.8	0.4	0.8	1.4
Kidney	1.8	3.3	4.7	1.5	2.9	4.4	0.6	1.3	2.1	0.5	1.0	1.6	0.4	0.9	1.6	0.4	0.8	1.4
Small intestine wall	0.9	1.6	2.4	0.3	0.6	0.9	0.1	0.3	0.5	0.1	0.2	0.4	0.1	0.3	0.5	0.1	0.2	0.3
Colon wall	1.9	3.5	4.9	0.3	0.6	1.0	0.1	0.3	0.5	0.1	0.2	0.4	0.1	0.2	0.3	0.1	0.2	0.3
Rectosigmoid wall	0.3	0.6	1.0	0.1	0.2	0.3	–	0.1	0.1	–	–	0.1	–	–	0.1	–	–	–
Urinary bladder wall	0.2	0.4	0.6	0.1	0.1	0.2	–	–	0.1	–	–	–	–	–	–	–	–	–
Prostate[b]	0.1	0.2	0.4	–	0.1	0.1	–	–	–	–	–	–	NA[d]	NA	NA	–	–	–
Uterus[b]	0.2	0.4	0.6	0.1	0.2	0.2	–	0.1	0.1	–	–	–	–	–	–	NA	NA	NA
Testes[b]	0.1	0.1	0.2	–	–	0.1	–	–	–	–	–	–	NA	NA	NA	–	–	–
Ovaries[b]	0.3	0.6	1.0	0.1	0.2	0.3	–	0.1	0.1	–	–	–	–	–	–	NA	NA	NA
Skin	2.4	4.1	5.6	1.5	2.6	3.6	1.1	2.0	2.7	1.0	1.7	2.4	0.9	1.5	2.1	0.9	1.5	2.2
Muscle	2.7	4.7	6.6	1.5	2.8	4.1	1.2	2.1	3.2	0.7	1.4	2.0	0.9	1.7	2.5	0.7	1.4	2.0
Active marrow	2.3	4.3	6.5	1.8	3.4	5.2	0.9	1.8	3.0	0.9	1.8	3.0	0.8	1.6	2.7	0.7	1.6	2.6
Shallow marrow	2.5	4.7	7.1	2.3	4.3	6.6	1.5	3.0	4.7	1.1	2.2	3.6	0.8	1.6	2.6	0.7	1.4	2.3
ED_{60}[c]	3.4	6.1	8.7	2.5	4.5	6.5	2.0	3.6	5.4	1.6	3.0	4.6	1.4	2.7	4.1			
ED_{103}[c]	3.9	6.9	9.9	2.8	5.1	7.4	2.3	4.2	6.1	1.9	3.5	5.3	1.6	3.0	4.6			

[a]Gender-independent organ doses for newborn, 1-year, 5-year, and 10-year phantoms were tabulated from male phantom since male and female phantoms have identical anatomy except gender-specific organs.
[b]Gender-specific organ doses were calculated separatelyfrom male and female phantoms.
[c]Effective doses were calculated using male and female organ doses as recommended by ICRP. Effective dose for 15-year phantoms was tabulated in 15-year female columns.
[d]Male organ doses are not available (NA) for 15-yearfemale phantom. Female organ doses are not available for 15-year male phantom.

TABLE IX. Organ absorbed doses (mGy/100 mAs) and effective doses (mSv/100 mAs) for newborn, 1-year, 5-year, 10-year, and 15-year male and female reference phantoms for **abdomen-pelvis CT examinations** using the Siemens SOMATOM Sensation 16 scanner model at tube potentials of 80, 100, and 120 kVp. The significant digits of table entries reflect the precision of the Monte Carlo calculations. Organ doses less than 0.1 mGy/100 mAs are not tabulated (indicated by a hyphen).

Abdomen-pelvis scan	Newborn[a]			1-year[a]			5-year[a]			10-year[a]			15-year Female			15-year-Male		
Tube Potential (kVp)	80 kVp	100 kVp	120 kVp	80 kVp	100 kVp	120 kVp	80 kVp	100 kVp	120 kVp	80 kVp	100 kVp	120 kVp	80 kVp	100 kVp	120 kVp	80 kVp	100 kVp	120 kVp
Brain	0.1	0.2	0.2	–	0.1	0.1	–	–	0.1	–	–	–	–	–	–	–	–	–
Pituitary gland	–	0.1	0.2	–	0.1	0.1	–	–	–	–	–	–	–	–	–	–	–	–
Lens	0.1	0.2	0.2	–	0.1	0.1	–	–	0.1	–	–	–	–	–	–	–	–	–
Eye balls	0.1	0.2	0.3	–	0.1	0.1	–	–	0.1	–	–	–	–	–	–	–	–	–
Salivary glands	0.3	0.6	1.0	0.1	0.2	0.4	0.1	0.1	0.2	–	0.1	0.1	–	–	0.1	–	–	–
Oral cavity	0.2	0.4	0.7	0.1	0.2	0.3	–	0.1	0.2	–	–	0.1	–	–	0.1	–	–	–
Spinal cord	4.0	7.2	10.5	3.1	5.8	8.6	2.5	4.8	7.5	1.8	3.6	5.7	1.1	2.3	3.8	1.4	2.8	4.4
Thyroid	0.4	0.8	1.2	0.3	0.6	1.0	0.2	0.3	0.5	0.1	0.2	0.3	0.1	0.1	0.2	0.0	0.1	0.2
Esophagus	2.9	5.3	7.7	1.3	2.4	3.7	1.3	2.6	4.1	0.9	1.9	3.1	0.9	1.8	3.0	0.7	1.5	2.5
Trachea	0.7	1.4	2.0	0.3	0.6	1.0	0.3	0.5	0.9	0.2	0.3	0.6	0.1	0.3	0.5	0.1	0.2	0.4
Thymus	0.9	1.6	2.5	0.6	1.2	1.9	0.4	0.8	1.3	0.2	0.5	0.8	0.1	0.3	0.5	0.1	0.2	0.4
Lungs	3.8	6.8	9.7	2.9	5.2	7.4	1.7	3.1	4.6	1.4	2.7	4.1	1.0	1.9	2.9	1.0	2.1	3.2
Breast	6.1	10.6	14.7	4.7	8.5	12.1	4.5	8.0	11.5	1.7	3.2	4.7	2.1	3.8	5.6	3.0	5.4	7.9
Heart wall	4.3	7.7	11.0	3.0	5.6	8.1	3.0	5.5	8.2	1.7	3.4	5.2	1.2	2.3	3.6	1.1	2.2	3.5
Stomach wall	6.6	11.8	17.0	5.3	9.8	14.5	5.0	9.3	13.8	4.2	8.1	12.4	4.0	7.6	11.6	3.3	6.4	9.9
Liver	6.8	12.1	17.1	5.7	10.4	15.1	5.0	9.3	13.8	4.2	8.0	12.1	3.9	7.5	11.4	3.4	6.7	10.3
Gall bladder	6.1	11.1	16.0	5.2	9.7	14.6	4.7	9.1	13.7	4.1	7.9	12.2	3.3	6.6	10.5	2.8	5.7	9.3
Adrenals	5.9	10.6	15.5	4.7	8.8	13.1	4.2	8.0	12.2	3.5	6.7	10.5	2.9	5.9	9.5	2.6	5.3	8.6
Spleen	6.8	12.0	17.0	6.0	10.7	15.3	5.1	9.5	13.8	4.7	8.6	12.7	4.2	7.8	11.4	3.6	6.8	10.2
Pancreas	6.6	11.9	17.0	5.5	10.1	15.0	4.8	9.1	13.9	3.7	7.4	11.7	3.3	6.7	10.7	2.6	5.3	8.7
Kidney	6.9	12.2	17.4	6.1	11.4	16.8	5.5	10.4	15.8	4.7	9.1	13.8	4.3	8.2	12.6	3.3	6.7	10.6
Small intestine wall	6.7	12.0	17.1	5.4	10.1	14.9	5.2	9.7	14.5	4.2	8.1	12.6	3.9	7.5	11.7	2.8	5.8	9.3
Colon wall	7.1	12.5	17.5	5.9	10.8	15.6	5.9	10.6	15.4	5.1	9.4	13.8	5.1	9.2	13.4	3.6	7.0	10.7
Rectosigmoid wall	5.8	10.4	15.2	4.3	8.0	12.2	3.7	7.1	10.9	3.1	6.1	9.7	2.4	4.9	8.0	2.0	4.1	6.6
Urinary bladder wall	6.4	11.3	15.7	4.9	9.1	13.7	4.5	8.2	12.0	3.3	6.4	9.8	2.1	4.2	6.7	1.7	3.5	5.7
Prostate[b]	4.1	7.2	10.4	2.8	5.1	7.7	0.9	1.8	2.8	0.8	1.7	2.7	NA[d]	NA	NA	0.4	0.8	1.4
Uterus[b]	5.4	9.9	14.3	4.1	7.8	12.0	3.6	7.0	11.1	2.9	5.9	9.5	2.0	4.3	7.1	NA	NA	NA
Testes[b]	0.9	1.6	2.3	1.0	1.8	2.7	0.6	1.1	1.8	0.3	0.7	1.2	NA	NA	NA	0.3	0.7	1.2
Ovaries[b]	5.7	10.4	14.9	5.1	9.4	14.1	4.4	8.3	12.8	3.4	6.7	10.8	2.7	5.4	8.8	NA	NA	NA
Skin	3.0	5.2	7.1	2.3	4.0	5.5	1.8	3.1	4.3	1.5	2.7	3.8	1.3	2.3	3.2	1.2	2.2	3.0
Muscle	4.4	7.8	10.9	2.6	4.9	7.2	2.0	3.7	5.4	1.4	2.5	3.8	1.4	2.6	3.9	1.3	2.4	3.6
Active marrow	1.8	3.5	5.4	1.7	3.3	5.3	1.0	2.1	3.5	1.2	2.5	4.2	1.3	2.7	4.7	1.0	2.2	3.8
Shallow marrow	2.0	3.8	5.7	2.3	4.5	7.0	1.6	3.2	5.1	1.3	2.7	4.5	1.1	2.4	3.9	0.8	1.8	3.0
ED_{60}[c]	4.4	7.8	11.2	3.6	6.7	9.8	3.1	5.7	8.7	2.5	4.7	7.4	2.1	4.1	6.3			
ED_{103}[c]	4.5	8.0	11.4	3.6	6.6	9.7	3.1	5.8	8.6	2.4	4.6	7.0	2.1	4.1	6.3			

[a]Gender-independent organ doses for newborn, 1-year, 5-year, and 10-year phantoms were tabulated from male phantom since male and female phantoms have identical anatomy except gender-specific organs.
[b]Gender-specific organ doses were calculated separatelyfrom male and female phantoms.
[c]Effective doses were calculated using male and female organ doses as recommended by ICRP. Effective dose for 15-year phantoms was tabulated in 15-year female columns.
[d]Male organ doses are not available (NA) for 15-yearfemale phantom. Female organ doses are not available for 15-year male phantom.

TABLE X. Organ absorbed doses (mGy/100 mAs) and effective doses (mSv/100 mAs) for newborn, 1-year, 5-year, 10-year, and 15-year male and female reference phantoms for chest-abdomen-pelvis (CAP) CT examinations using the Siemens SOMATOM Sensation 16 scanner model at tube potentials of 80, 100, and 120 kVp. The significant digits of table entries reflect the precision of the Monte Carlo calculations. Organ doses less than 0.1 mGy/100 mAs are not tabulated (indicated by a hyphen).

CAP scan	Newborn[a]			1-year[a]			5-year[a]			10-year[a]			15-year-Female			15-year-male		
Tube potential (kVp)	80 kVp	100 kVp	120 kVp	80 kVp	100 kVp	120 kVp	80 kVp	100 kVp	120 kVp	80 kVp	100 kVp	120 kVp	80 kVp	100 kVp	120 kVp	80 kVp	100 kVp	120 kVp
Brain	0.3	0.5	0.8	0.1	0.3	0.5	0.1	0.2	0.3	0.1	0.2	0.3	0.1	0.1	0.2	–	0.1	0.2
Pituitary gland	0.3	0.5	0.8	0.1	0.3	0.5	0.1	0.2	0.2	0.1	0.1	0.3	–	0.1	0.2	–	0.1	0.1
Lens	0.3	0.5	0.8	0.1	0.2	0.4	0.1	0.1	0.2	–	0.1	0.2	–	0.1	0.2	0.1	0.1	0.2
Eye balls	0.3	0.5	0.9	0.1	0.2	0.4	0.1	0.1	0.2	0.1	0.1	0.2	–	0.1	0.2	–	0.1	0.2
Salivary glands	4.2	7.4	10.6	0.9	1.6	2.4	0.5	0.9	1.4	0.4	0.9	1.4	0.3	0.5	0.8	0.2	0.4	0.7
Oral cavity	1.9	3.5	5.0	0.5	1.0	1.6	0.3	0.6	1.0	0.3	0.6	0.9	0.3	0.6	0.9	0.2	0.4	0.7
Spinal cord	6.1	11.0	16.0	4.9	9.0	13.4	3.9	7.6	11.9	2.5	4.9	7.8	2.2	4.4	7.2	1.9	3.9	6.3
Thyroid	7.3	12.9	18.1	6.2	11.0	15.8	6.1	10.8	15.0	4.8	8.4	11.9	3.5	6.3	9.1	3.1	5.8	8.4
Esophagus	5.9	10.7	15.7	4.8	8.9	13.4	4.2	7.9	12.2	3.4	6.6	10.6	2.8	5.6	8.9	2.5	5.2	8.4
Trachea	6.0	10.8	15.7	5.5	9.9	14.6	5.1	9.3	13.8	3.7	7.1	11.1	3.3	6.5	10.1	3.0	5.9	9.3
Thymus	6.3	11.3	16.1	5.7	10.4	15.3	5.5	10.1	14.7	4.1	7.9	12.2	3.6	7.0	10.9	3.2	6.3	10.0
Lungs	6.9	12.2	17.4	6.6	11.8	16.9	5.6	10.2	14.9	4.7	8.9	13.3	3.8	7.3	11.1	3.6	7.0	10.8
Breast	6.7	11.6	16.2	5.2	9.4	13.5	4.8	8.6	12.5	4.1	7.5	10.9	3.7	6.8	9.9	3.6	6.6	9.7
Heart wall	7.1	12.7	18.0	6.5	11.8	17.2	5.8	10.7	15.8	4.8	9.1	13.9	4.1	7.8	12.0	3.9	7.6	11.7
Stomach wall	6.9	12.3	17.8	5.8	10.7	15.8	5.3	9.9	14.8	4.5	8.7	13.3	4.3	8.1	12.4	3.4	6.8	10.7
Liver	7.2	12.9	18.3	6.1	11.3	16.4	5.4	10.1	15.0	4.7	8.9	13.5	4.2	8.2	12.5	3.7	7.2	11.2
Gall bladder	6.3	11.4	16.6	5.4	10.1	15.3	4.8	9.3	14.1	4.2	8.2	12.8	3.4	6.9	11.2	2.9	6.0	9.8
Adrenals	6.1	11.1	16.2	5.3	9.8	14.7	4.5	8.7	13.3	3.7	7.3	11.5	3.1	6.4	10.2	2.8	5.8	9.4
Spleen	7.2	12.7	18.0	6.5	11.6	16.7	5.5	10.2	14.9	5.0	9.2	13.6	4.4	8.3	12.3	3.8	7.2	10.9
Pancreas	6.8	12.2	17.6	5.6	10.4	15.5	4.9	9.4	14.4	3.9	7.7	12.2	3.4	6.9	11.1	2.6	5.5	9.0
Kidney	7.0	12.5	17.9	6.4	11.9	17.6	5.7	10.8	16.3	4.9	9.3	14.3	4.3	8.4	13.0	3.4	6.9	10.9
Small intestine wall	6.8	12.1	17.3	5.5	10.2	15.1	5.3	9.9	14.8	4.2	8.2	12.7	3.9	7.6	11.8	2.8	5.8	9.4
Colon wall	7.2	12.7	17.7	6.0	10.9	15.8	5.9	10.8	15.6	5.1	9.4	13.9	5.1	9.3	13.5	3.6	7.0	10.8
Rectosigmoid wall	5.8	10.5	15.3	4.3	8.1	12.3	4.0	7.7	11.8	3.1	6.1	9.7	2.4	5.0	8.0	2.0	4.1	6.6
Urinary bladder wall	6.5	11.3	15.8	5.0	9.2	13.7	5.3	9.7	14.0	3.3	6.4	9.8	2.1	4.2	6.7	1.7	3.5	5.7
Prostate[b]	4.1	7.3	10.4	2.8	5.1	7.7	1.3	2.5	3.9	0.8	1.7	2.7	NA[d]	NA	NA	0.4	0.8	1.4
Uterus[a]	5.5	10.0	14.4	4.1	7.9	12.1	3.8	7.4	11.6	2.9	5.9	9.5	2.0	4.3	7.1	NA	NA	NA
Testes[a]	0.9	1.6	2.4	1.0	1.9	2.7	0.8	1.5	2.3	0.3	0.7	1.2	NA	NA	NA	0.3	0.7	1.2
Ovaries[a]	5.7	10.4	15.1	5.1	9.5	14.2	4.6	8.7	13.3	3.4	6.7	10.8	2.7	5.4	8.8	NA	NA	NA
Skin	4.1	7.0	9.6	3.2	5.5	7.6	2.5	4.5	6.2	2.3	4.0	5.5	1.9	3.3	4.6	1.8	3.3	4.5
Muscle	5.4	9.5	13.4	3.5	6.4	9.3	2.7	5.0	7.4	1.9	3.5	5.1	2.0	3.7	5.5	1.8	3.3	4.9
Active marrow	3.1	5.9	9.0	2.8	5.4	8.5	1.7	3.5	5.8	1.9	3.9	6.5	1.8	3.9	6.6	1.6	3.3	5.7
Shallow marrow	3.4	6.4	9.7	3.8	7.3	11.3	2.8	5.6	8.9	2.2	4.5	7.3	1.7	3.6	5.9	1.4	2.9	4.7
ED_{60}[c]	5.5	9.9	14.2	4.8	8.9	13.1	4.3	7.9	11.9	3.5	6.7	10.3	2.9	5.6	8.6			
ED_{103}[c]	5.7	10.2	14.5	4.8	8.8	13.0	4.3	7.9	11.8	3.6	6.8	10.4	3.0	5.7	8.8			

[a]Gender-independent organ doses for newborn, 1-year, 5-year, and 10-year phantoms were tabulated from male phantom since male and female phantoms have identical anatomy except gender-specific organs.
[b]Gender-specific organ doses were calculated separately from male and female phantoms.
[c]Effective doses were calculated using male and female organ doses as recommended by ICRP. Effective dose for 15-year phantoms was tabulated in 15-year female columns.
[d]Male organ doses are not available (NA) for 15-year female phantom. Female organ doses are not available for 15-year male phantom.

four major scan types were calculated by using the $CTDI_{vol}$ measurements (see Sec. II.D) and the normalized values given in Tables III–VI. The resulting organ and effective doses (mGy/100 mAs) for the newborn, 1, 5, 10, and 15-year male and female phantoms were tabulated in Tables VII–X for the tube potential of 80, 100, and 120 kVp. It must be noted that the following analysis is valid under the assumption that the same mAs is used even for different body sizes.

In the head scan as shown in Table VII, brain and eye lens receive significant doses. Brain and eye lens of the 15-year male phantom receive 11.6 and 14.0 mGy/100mAs, respectively, for the tube potential of 120 kVp. The brain of the newborn receives 15.8 mGy/100 mAs at 120 kVp which is 1.4-fold greater than that seen in the 15-year male. As compared to its value at 80 kVp, the ratio of brain doses in the newborn to those of 15-year-old phantoms are 2.5- to 3-fold greater at a tube potential of 120 kVp. Salivary gland dose increases for the head scan at older ages, which is opposite to that seen for other organs. If an organ is fully included within the scan range (e.g., brain), the radiation incident to the organ experiences greater attenuation in the older phantoms than in younger phantoms which results in a lower organ dose in the older phantoms. The higher salivary gland dose in older phantoms is partly caused by the increasing portion of salivary glands included within the head scan. ED_{103} is shown to be very comparable with ED_{60} across all tube potentials and ages. ED_{60} is slightly greater than ED_{103} in the newborn and 1-year phantoms but ED_{60} for the 5, 10, and 15-year phantoms is smaller than ED_{60}. ICRP Publication 60 states that when a single one of the remainder organs receives an equivalent dose in excess of the highest dose in any of the twelve organs for which a weighting factor is specified, a tissue weighting factor of 0.025 should be applied to the organ and the value of 0.025 to the average dose in the rest of the remainder. This is the case in the head examination in the CT scan which gives the highest dose to brain among the organs to which tissue weighting factors are given. Hence, the tissue weighting factors of 0.025 and 0.01 are assigned to brain according to ICRP 60 and ICRP 103, respectively, which results in higher ED_{60} than ED_{103} over all ages. However, since a new tissue weighting factor of 0.01 is now assigned to the salivary glands within which the absorbed dose changes from one half the brain dose in the newborn to an equivalent value of the brain dose in 15-year phantom, ED_{103} increases and becomes higher than ED_{60} in the phantoms at ages above 5 years.

The heart wall at all ages receives the greatest dose under chest CT scans as given in Table VIII. The heart wall in the newborn phantom receives 17.3 mGy/100mAs at 120 kVp which is 1.5-fold greater than the heart wall dose in the 15-year phantom. Lungs and thymus received slightly smaller doses than seen for the heart wall. The ED_{103} is 1.14-fold greater than the ED_{60} on average for different ages and tube potentials. This is partly attributed to the increase of the tissue weighting factor of the breast from 0.05 (ICRP 60) to 0.12 (ICRP 103).

As for the abdomen–pelvis scan in Table IX, kidneys and colon receive the highest doses around 10.6 and 10.7 mGy/100 mAs (15-year male and 120 kVp), respectively, which are followed by a group of organs receiving similar dose levels from 9 to 10 mGy/100 mAs (15-year male and 120 kVp): small intestine, spleen, pancreas, gall bladder, stomach, and liver. The two major organ groups in the newborn receive 17.4 (kidney) and 17.5 (colon), respectively. The ED_{60} is almost comparable with ED_{103} in the abdomen–pelvis scans since the

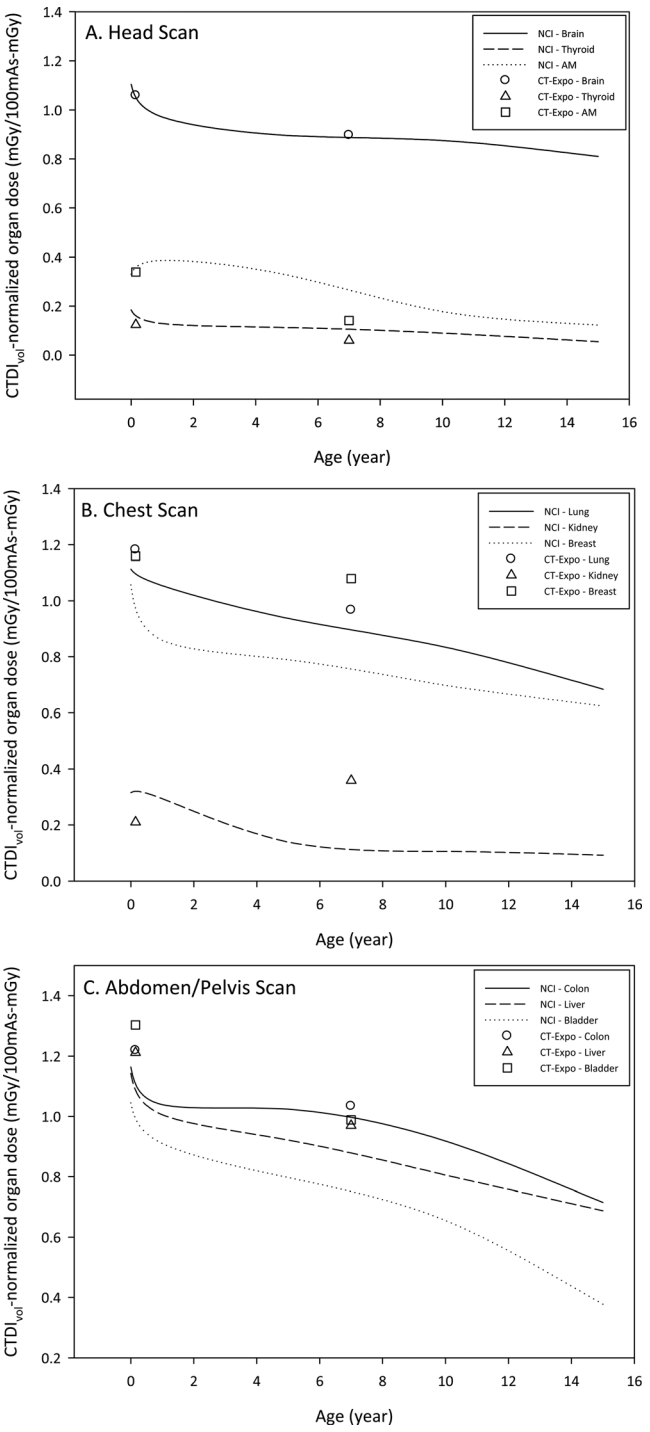

FIG. 2. The comparison of organ doses normalized by $CTDI_{vol}$ for (a) head scan (brain, thyroid, and active marrow), (b) chest scan (lung, kidney, and breast), and (c) abdomen/pelvis scan (colon, liver, and urinary bladder) between the CT-Expo and the NCI calculations.

TABLE XI. Comparison of major organ doses (mGy/100 mAs mGy) for the organs completely included in the abdomen/pelvis scan as derived by empirical correlation with patient abdominal circumference (Turner *et al.*) and as calculated from the organ dose matrix of the present study.

		Regression coefficients		Age (year)					
	Organs	A_0	B_0	0	1	5	10	15F	15M
Turner et al.	Liver	3.8240	−0.0120	2.45	2.02	1.91	1.63	1.41	1.33
	Stomach	3.7800	−0.0113	2.49	2.08	1.96	1.69	1.48	1.40
	Adrenals	4.0290	−0.0128	2.51	2.04	1.92	1.62	1.39	1.31
	Kidney	3.9690	−0.0124	2.51	2.06	1.93	1.65	1.42	1.33
	Pancreas	3.7150	−0.0122	2.37	1.95	1.83	1.56	1.35	1.27
	Spleen	3.5140	−0.0111	2.33	1.95	1.85	1.60	1.40	1.32
	Gall bladder	3.9940	−0.0115	2.61	2.17	2.05	1.77	1.54	1.45
Our study	Liver			2.30	2.03	1.85	1.62	1.53	1.38
	Stomach			2.28	1.95	1.85	1.66	1.56	1.33
	Adrenals			2.07	1.75	1.64	1.41	1.27	1.16
	Kidney			2.34	2.26	2.12	1.86	1.70	1.42
	Pancreas			2.28	2.01	1.87	1.57	1.43	1.16
	Spleen			2.28	2.06	1.85	1.70	1.54	1.37
	Gall bladder			2.15	1.97	1.84	1.64	1.41	1.25

TABLE XII. Comparison of effective doses normalized to dose length product (DLP) (mSv/mGy cm) as given by Shrimpton *et al.* and as calculated using the dose matrix of the present study under either ICRP 60 or ICRP 103 tissue weighting factors.

			Age (year)					
	Scan type	kVp	0	1	5	10	15	30
Shrimpton *et al.*[a]	Head	120	0.0110	0.0067	0.0040	0.0032		0.0021
	Chest		0.0390	0.0260	0.0180	0.0130		0.0140
	Abdomen/peivls		0.0490	0.0300	0.0200	0.0150		0.0150
	Trunk		0.0440	0.0280	0.0190	0.0140		0.0150
NCI ED60	Head	80	0.0084	0.0049	0.0033	0.0023	0.0016	0.0013
		100	0.0085	0.0054	0.0037	0.0026	0.0018	0.0015
		120	0.0092	0.0060	0.0043	0.0029	0.0021	0.0017
	Chest	80	0.0428	0.0268	0.0190	0.0126	0.0087	0.0168
		100	0.0432	0.0277	0.0198	0.0134	0.0096	0.0180
		120	0.0446	0.0291	0.0210	0.0146	0.0106	0.0186
	Abdomen/Pelvis	80	0.0447	0.0283	0.0193	0.0122	0.0093	0.0195
		100	0.0451	0.0294	0.0203	0.0132	0.0102	0.0210
		120	0.0465	0.0313	0.0222	0.0149	0.0114	0.0219
	CAP	80	0.0413	0.0261	0.0184	0.0120	0.0087	0.0155
		100	0.0417	0.0274	0.0193	0.0129	0.0095	0.0168
		120	0.0430	0.0290	0.0208	0.0144	0.0106	0.0175
NCI ED103	Head	80	0.0075	0.0048	0.0034	0.0023	0.0017	0.0013
		100	0.0079	0.0052	0.0038	0.0026	0.0019	0.0015
		120	0.0086	0.0058	0.0043	0.0029	0.0022	0.0017
	Chest	80	0.0492	0.0306	0.0219	0.0146	0.0103	0.0191
		100	0.0494	0.0315	0.0227	0.0155	0.0110	0.0203
		120	0.0508	0.0330	0.0240	0.0168	0.0121	0.0210
	Abdomen/pelvis	80	0.0460	0.0281	0.0198	0.0120	0.0094	0.0159
		100	0.0463	0.0292	0.0207	0.0129	0.0103	0.0172
		120	0.0475	0.0309	0.0221	0.0142	0.0114	0.0179
	CAP	80	0.0425	0.0263	0.0186	0.0123	0.0089	0.0162
		100	0.0428	0.0273	0.0194	0.0132	0.0097	0.0173
		120	0.0440	0.0288	0.0207	0.0144	0.0108	0.0180

[a]Tissue weighting factors in ICRP60 were adopted to calculate effective doses in Shrimpton *et al.*

effective dose increase caused by the change in the breast tissue weighting factor (0.05 of ICRP60 to 0.12 of ICRP103) is compensated by the decrease of the gonadal tissue weighting factor (0.2 of ICRP60 to 0.08 of ICRP103). A similar trend of ED_{60} and ED_{103} is also observed in the organ doses for the CAP scan tabulated in Table X where breast and gonad doses majorly contribute to the effective dose.

III.C. Comparison of pediatric organ doses with other data

III.C.1. Comparison with CT-Expo

The selected organ doses were compared with the values obtained from CT-Expo. It is very difficult to define scan start, scan end, and scan range in the pediatric phantoms of CT-Expo using their anatomical landmarks. Although the 2-month and 7-year-old GSF voxel phantoms were used in the dose calculation, the program provides only a graphical display of stylized organ anatomy for users to define the scan range.[12] Thus, the stylistic diagram in the CT-Expo was used to define the scan ranges since the anatomy of the original voxel phantoms is not available. Scan ranges for head, chest, and abdomen–pelvis studies were defined in the CT-Expo by using the identical anatomical landmarks used in the NCI calculations (see Sec. II.D). The scan range in the CT-Expo program for head, chest, abdominalpelvis, and CAP examinations was defined as from the top of the head to the bottom of the cranium (surrogate for 2nd cervical vertebra), from the top of the trunk (surrogate for the clavicles) to the middle of the liver, and from the top of the liver to the bottom of the pelvis (surrogate for the to the midfemoral head), respectively. The dose comparison is depicted in Fig. 2.

As for the head scan, the organ doses for brain, thyroid, and active marrow were compared between our study (denoted as NCI in the graphs) and CT-Expo. Although brain and thyroid doses show no significant differences as in Fig. 2(a), active marrow dose in 7-year child in CT-expo is almost half of the value from the NCI calculation. In case of the chest scan shown in Fig. 2(b), lung doses do not show a significant difference between the NCI calculations and the CT-Expo results, whereas the doses to the breasts and kidneys are substantially different especially for the 7-year-old child. The breasts and kidneys of the 7-year-old child in the CT-Expo receive 1.5-fold and 2.9-fold greater dose than those for the 7-year-old child, respectively, which can be interpolated from the 5- and 10-year-old phantoms. Figure 2(c) shows the comparison of the doses to colon, liver, and urinary bladder in the abdomen–pelvis scan between the

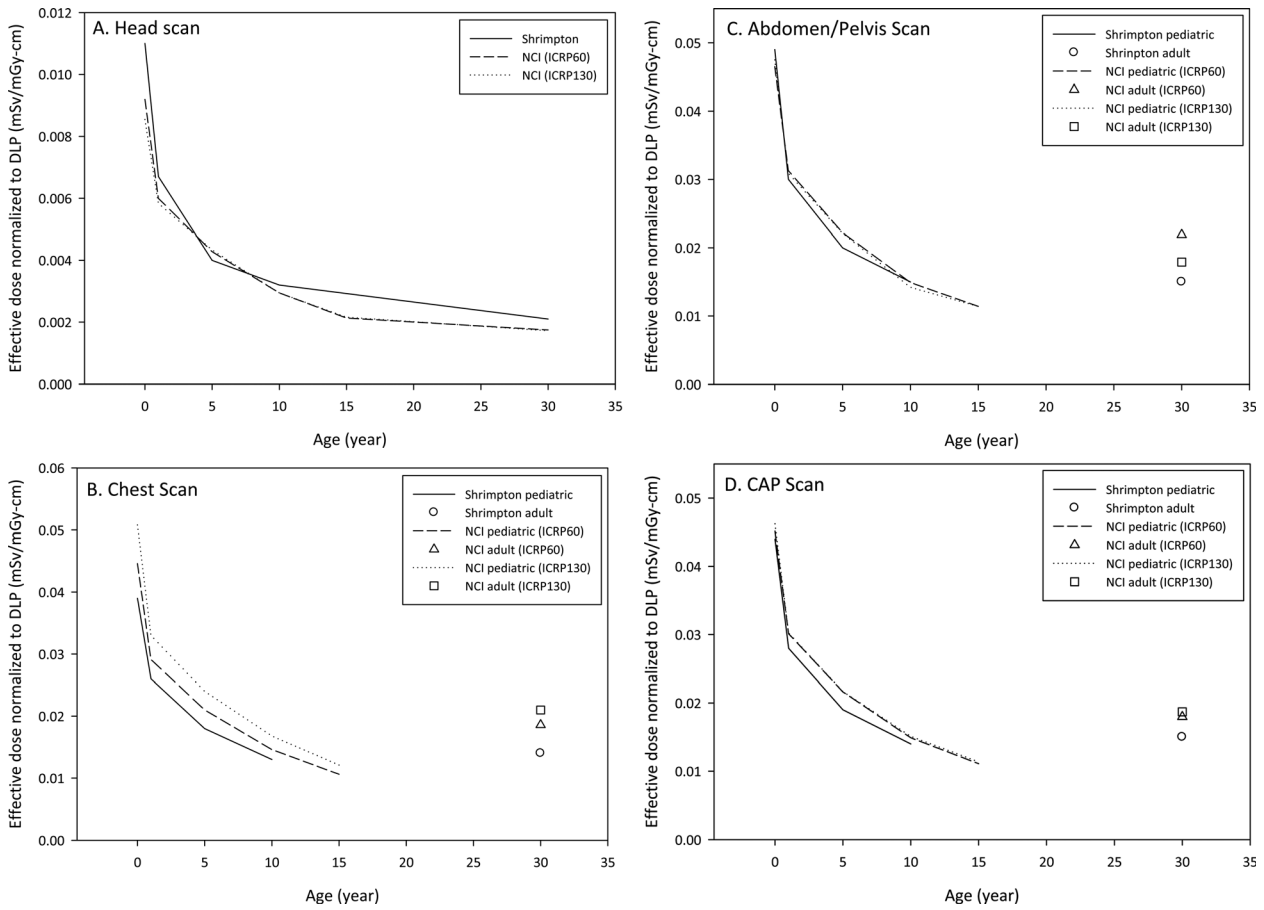

FIG. 3. Comparison of effective dose normalized to DLP (mSv/mGy cm) for pediatric and adult reference individuals undergoing (a) head, (b) chest, (c) abdomen/pelvis, and (d) CAP scans between Shrimpton *et al*. and the calculations in this study.

NCI calculations and CT-Expo. Although colon and liver do not show significant differences, urinary bladder of the 7-year-old child in CT-Expo received around 1.3-fold greater dose than seen in the NCI calculations. The discrepancies observed in the chest and abdomen–pelvis scans are likely attributed to the difficulties in correctly defining the scan ranges within the CT-Expo.

III.C.2. Comparison with organ doses derived from circumference

The absorbed doses to selected organs were also calculated using the regression coefficients provided in Turner *et al*.[24] These values were compared with those calculated from our study as tabulated in Table XI. For the liver, stomach, pancreas, and spleen in each pediatric phantom, the doses calculated using the Turner *et al*. method fell within 10% of those explicitly calculated in this study. The kidney doses remained within 10% for all phantoms except for the 10-year-old and 15-year-old female, which had percent differences of 11.3% and 16.5%, respectively. The greatest differences were seen in the adrenals and gall bladder doses, which were all overestimated by the Turner method for every phantom, especially in the newborn. For the newborn, the percent differences from the explicitly calculated adrenals and gall bladder doses rose to 21%. Overall, the data seem to support that the reference body sizes corresponding to the age of the phantoms acceptably follows the correlation between the body circumference and the organ dose. However, the method is only valid for abdomen–pelvis scans.

III.C.3. Comparison with the existing DLP-to-effective dose conversion coefficients

The effective doses, ED_{60} and ED_{103}, calculated in this study were normalized to the DLP and compared with the existing DLP-to-effective dose conversion coefficients based on the tissue weighting factors from ICRP 60 and derived from stylized phantoms.[25] The comparison is tabulated in Table XII and also depicted in Fig. 3. When ED_{60} from this study was compared with the existing coefficients, the overall trend showed that the existing conversion coefficients tended to be smaller than the normalized effective doses from the present study for all examinations except head scans where the existing coefficients are up to 1.17 fold greater than those in this study (the one exception being the 5-year-old phantom). The abdomen–pelvis exam coefficients differed greatest from those calculated in this study over all phantom ages: our coefficient is up to 1.5 fold greater than the published values. Overall, the coefficients most poorly matched were those of the adult phantoms. The majority of these differences can easily be attributed to the vast differences in anatomical accuracy between the stylized phantoms used in the Shrimpton *et al*. study and the hybrid phantoms used in the present study. Similar to the Turner *et al*. method, the use of the Shrimpton coefficients could potentially be used for quick, less accurate effective dose estimations for certain cases. However, based on the data in this study, these coefficients would be inadvisable especially for chest exams and for adult patients.

IV. CONCLUSIONS

A comprehensive organ/effective dose database was established using Monte Carlo simulation of a CT scanner and a series of computational reference human phantoms ranging from newborn to 15-year-old male and female. The database covers a total of 33 organs and tissues including active marrow, three tube potentials (80, 100, and 120 kVp), and both head and body filters. The comparisons of our results with the three independent existing studies reveal that use of phantoms with realistic anatomy is crucial to improved accuracy in CT organ dosimetry. The 5D organ dose matrix developed in this study is the first organ-specific pediatric CT scan database based on a series of realistic pediatric hybrid phantoms that are compliant with the organ mass and body sizes reported by the ICRP.

Nevertheless, there are a couple of limitations in this study which should be taken care of in the future. We did not account for the variation of the body size even within the patients of the same age. A library of phantoms with different body sizes which is feasible by using hybrid phantom technique will be incorporated into the database to take this variation into account in the future. Some components within the Eq. (1) must be verified such as the estimation of the dose from helical scan by the summation of the dose from axial scans. Although the organ dose data can be utilized for basic CT imaging techniques, more recent technologies such as tube current modulation,[26–28] dual source scanning,[29] and the collimation other than 10 mm were not included in the dose calculation. A series of further modeling and dose calculations will be incorporated into the organ dose matrix to better account for these different imaging techniques.

Organ- or tissue-specific estimated doses for large numbers of exposed individuals are essential for epidemiologic studies of radiation exposure to CT examinations and provide the critical data required for modeling radiation dose response. In many cases, the near-field organs and tissues are of particular interest in the epidemiologic studies. The organ dose database developed in this study is very unique tool for the epidemiologic studies, of which features cannot be provided by any existing data or software programs. The organ dose database established for pediatric phantoms is being coupled with the adult organ dose database recently published to develop a user-friendly computer program that will enable rapid estimates of organ and effective dose doses for patients of any age, gender, examination types, and CT scanner model.

ACKNOWLEDGMENTS

This work was supported by Contract Nos. HHS-N2612-0090-0098P, HHS-N2612-0100-0692P, and HHS-N2612-0090-0177P with the Radiation Epidemiology Branch of the National Cancer Institute.

[a]Author to whom correspondence should be addressed. Electronic mail: leechoonsik@mail.nih.gov. Telephone: (301)-443-8224; Fax: (301)-402-0207.

[1]D. J. Brenner and E. J. Hall, "Computed tomography—An increasing source of radiation exposure," N. Engl. J. Med. **357**, 2277–2284 (2007).

[2]A. Berrington de Gonzalez, M. Mahesh, K. P. Kim, M. Bhargavan, R. Lewis, F. Mettler, and C. Land, "Projected cancer risks from computed tomographic scans performed in the United States in 2007," Arch. Intern. Med. **169**, 2071–2077 (2009).
[3]NCRP. *Ionizing Radiation Exposure of the Population of the United States*. Bethesda, MD, National Council on Radiation Protection and Measurement, 2009.
[4]M. Goske, K. Applegate, J. Boylan, P. Butler, M. Callahan, B. Coley, S. Farley, D. Frush, M. Hernanz-Schulman, and D. Jaramillo, "The image gently campaign: Working together to change practice," Am. J. Roentgenol. **190**, 273–274 (2008).
[5]http://www.fda.gov/NewsEvents/Newsroom/PressAnnouncements/UCM200085.
[6]M. Cristy and K. F. Eckerman, Report No. ORNL/TM-8381, Vol. 1–7 (1987).
[7]A. Khursheed, M. Hillier, P. Shrimpton, and B. Wall, "Influence of patient age on normalized effective doses calculated for CT examinations," Br. J. Radiol. **75**, 819–830 (2002).
[8]M. Zankl, W. Panzer, N. Petoussi-Henss, and G. Drexler, "Organ doses for children from computed tomographic examinations," Radiat. Prot. Dosim. **57**, 393–396 (1995).
[9]R. J. Staton, C. Lee, C. Lee, M. D. Williams, D. E. Hintenlang, M. M. Arreola, J. L. Williams, and W. E. Bolch, "Organ and effective doses in newborn patients during helical multislice computed tomography examination," Phys. Med. Biol. **51**, 5151–5166 (2006).
[10]C. Lee, C. Lee, R. J. Staton, D. E. Hintenlang, M. M. Arreola, J. L. Williams, and W. E. Bolch, "Organ and effective doses in pediatric patients undergoing helical multislice computed tomography examination," Med. Phys. **34**, 1858–1873 (2007).
[11]X. Li, E. Samei, W. P. Segars, G. M. Sturgeon, J. G. Colsher, G. Toncheva, T. T. Yoshizumi, and D. P. Frush, "Patient-specific radiation dose and cancer risk estimation in CT: Part II. Application to patients," Med. Phys. **38**, 408 (2011).
[12]G. Stamm and H. D. Nagel, "CT-expo—A novel program for dose evaluation in CT," RöFo: Fortschritte auf dem Gebiete der Röntgenstrahlen und der Nuklearmedizin **174**, 1570–1576 (2002).
[13]D. B. Pelowitz, Report No. LA-CP-05-0369 (2008).
[14]C. Lee, K. Kim, D. Long, R. Fisher, C. Tien, S. Simon, A. Bouville, and W. Bolch, "Organ doses for reference adult male and female undergoing computed tomography estimated by Monte Carlo simulations," Med. Phys. **38**, 1196–1206 (2011).
[15]G. Jarry, J. J. DeMarco, U. Beifuss, C. H. Cagnon, and M. F. McNitt-Gray, "A Monte Carlo-based method to estimate radiation dose from spiral CT: from phantom testing to patient-specific models," Phys. Med. Biol. **48**, 2645–2663 (2003).
[16]C. Lee, D. Lodwick, J. Hurtado, D. Pafundi, J. L. Williams, and W. E. Bolch, "The UF family of reference hybrid phantoms for computational radiation dosimetry," Phys. Med. Biol. **55**, 339–363 (2010).
[17]C. Lee, C. Lee, D. Lodwick, and W. E. Bolch, "Development of hybrid computational phantoms of newborn male and female for dosimetry calculation," Phys. Med. Biol. **52**, 3309–3333 (2007).
[18]C. Lee, D. Lodwick, J. L. Williams, and W. E. Bolch, "Hybrid computational phantoms of the 15-year male and female adolescent: Applications to CT organ dosimetry for patients of variable morphometry," Med. Phys. **35**, 2366–2382 (2008).
[19]ICRP, "Basic anatomical and physiological data for use in radiological protection: reference values," ICRP publication 89 (International Commission on Radiological Protection, Oxford, 2003).
[20]ICRU, "Proton and Neutron Interaction Data for Body Tissues," ICRU report 46 (International Commission on Radiation Units and Measurements, 1992).
[21]ICRP, "Human alimentary tract model for radiological protection," ICRP Publication 100 (International Commission on Radiological Protection, Oxford, Pergamon Press, 2006).
[22]P. B. Johnson, A. A. Bahadori, K. F. Eckerman, C. Lee, and W. E. Bolch, "Response functions for computing absorbed dose to skeletal tissues from photon irradiation—An update," Phys. Med. Biol. **56**, 2347 (2011).
[23]A. C. Turner, M. Zankl, J. J. DeMarco, C. H. Cagnon, D. Zhang, E. Angel, D. D. Cody, D. M. Stevens, C. H. McCollough, and M. F. McNitt-Gray, "The feasibility of a scanner-independent technique to estimate organ dose from MDCT scans: using CTDIvol to account for differences between scanners," Med. Phys. **37**, 1816–1825 (2010).
[24]A. C. Turner, D. Zhang, M. Khatonabadi, M. Zankl, J. J. DeMarco, C. H. Cagnon, D. D. Cody, D. M. Stevens, C. H. McCollough, and M. F. McNitt-Gray, "The feasibility of patient size-corrected, scanner-independent organ dose estimates for abdominal CT exams," Med. Phys. **38**, 820–829 (2011).
[25]C. McCollough, D. Cody, S. Edyvean, R. Geise, B. Gould, N. Keat, W. Huda, P. Judy, W. Kalender, and M. McNitt-Gray, *The measurement, Reporting, and Management of Radiation Dose in CT* (American Association of Physicists in Medicine, College Park, MD, 2008).
[26]E. Angel, N. Yaghmai, C. M. Jude, J. J. Demarco, C. H. Cagnon, J. G. Goldin, A. N. Primak, D. M. Stevens, D. D. Cody, C. H. McCollough, and M. F. McNitt-Gray, "Monte Carlo simulations to assess the effects of tube current modulation on breast dose for multidetector CT," Phys. Med. Biol. **54**, 497–512 (2009).
[27]H. Schlattl, M. Zankl, J. Becker, and C. Hoeschen, "Dose conversion coefficients for CT examinations of adults with automatic tube current modulation," Phys. Med. Biol. **55**, 6243–6261 (2010).
[28]M. van Straten, P. Deak, P. C. Shrimpton, and W. A. Kalender, "The effect of angular and longitudinal tube current modulations on the estimation of organ and effective doses in x-ray computed tomography," Med. Phys. **36**, 4881–4889 (2009).
[29]M. Petersilka, H. Bruder, B. Krauss, K. Stierstorfer, and T. G. Flohr, "Technical principles of dual source CT," Eur. J. Radiol. **68**, 362–368 (2008).
[30]http://www.cdc.gov/nchs/nhanes.htm
[31]https://projects.ctrip.ufl.edu/protocols/snips/